

From Hierarchical to Partially Degenerate Neutrinos via Type II Upgrade of Type I See-Saw Models

S. Antusch¹, S. F. King²

*Department of Physics and Astronomy, University of Southampton,
Southampton, SO17 1BJ, U.K.*

Abstract

We propose a type II upgrade of type I see-saw models leading to new classes of models where partially degenerate neutrinos are as natural as hierarchical ones. The additional type II contribution to the neutrino mass matrix, which determines the neutrino mass scale, is forced to be proportional to the unit matrix by a $SO(3)$ flavour symmetry. The type I see-saw part of the neutrino mass matrix, which controls the mass squared differences and mixing angles, may be governed by sequential right-handed neutrino dominance and a natural alignment for the $SO(3)$ -breaking vacuum. We focus on classes of models with bi-large mixing originating from the neutrino mass matrix although we also briefly discuss other classes of models where large mixing stems from the charged lepton mass matrix. We study renormalization group corrections to the neutrino mass squared differences and mixings and find that the low energy values do not depend sensitively on the high energy values for partially degenerate neutrinos with a mass scale up to about 0.15 eV. Our scenario predicts the effective mass for neutrinoless double beta decay to be approximately equal to the neutrino mass scale and therefore neutrinoless double beta decay will be observable if the neutrino mass spectrum is partially degenerate. We also find that all observable CP phases as well as θ_{13} become small as the neutrino mass scale increases.

¹E-mail: santusch@hep.phys.soton.ac.uk

²E-mail: sfk@hep.phys.soton.ac.uk

1 Introduction

The observation of flavour conversions of neutrinos together with their interpretation by neutrino oscillations has brought crucial new information about fermion masses and mixings. Neutrinos are massive, with very small measured mass squared differences, and contrary to the quark sector, there is large flavour mixing among the leptons. The present 3σ ranges for the parameters are $\theta_{12} \in [27.6^\circ, 36.3^\circ]$, $\Delta m_{\text{sol}}^2 := m_2^2 - m_1^2 \in [5.4 \cdot 10^{-5} \text{ eV}^2, 9.5 \cdot 10^{-5} \text{ eV}^2]$, $\theta_{23} \in [32.2^\circ, 51.4^\circ]$, $|\Delta m_{\text{atm}}^2| := |m_3^2 - m_1^2| \in [1.4 \cdot 10^{-3} \text{ eV}^2, 3.7 \cdot 10^{-3} \text{ eV}^2]$ and for θ_{13} the current upper bound which mainly stems from the CHOOZ data [1] is $\theta_{13} \lesssim 15^\circ$. The values have been taken from the global analysis [2] which includes the the Super-Kamiokande atmospheric data [3], the KamLAND results [4] and recent SNO salt results [5].

One of the most interesting missing piece of information is the neutrino mass scale. At present, the most stringent bounds are $m_i < 0.23 \text{ eV}$ from WMAP [6] and $\langle m_\nu \rangle \lesssim 0.35 \text{ eV}$, with some uncertainty due to nuclear matrix elements, from neutrino-less double beta ($00\nu\beta\beta$) decay experiments [7, 8]. The latter search for an effective mass defined by $\langle m_\nu \rangle = |\sum_i (U_{\text{MNS}})_{1i}^2 m_i|$ and are exclusively sensitive to Majorana masses. Future experiments which are under consideration at present might increase the sensitivity to $\langle m_\nu \rangle$ by more than an order of magnitude. The neutrino mass spectrum for the mass range accessible to this next round of $0\nu\beta\beta$ decay searches shows at least a partial degeneracy. It is therefore interesting to investigate theoretical scenarios which could account for such neutrino mass schemes.

The most promising scenarios for giving masses to neutrinos use a version of the see-saw mechanism [9, 10, 11, 12], which provides a convincing explanation for their smallness. Models for strongly degenerate neutrinos have been considered e.g. in [13, 14, 15, 16, 17, 18, 19, 20, 21, 22, 23, 24, 25, 26, 27, 28, 29, 30, 31, 32, 33]. In most of them, the degeneracy is achieved by discrete symmetries. The non-Abelian flavour symmetry group $\text{SO}(3)$ in connection with degenerate neutrinos has e.g. been considered in [25, 20, 21, 24, 27]. It has turned out that using the type I see-saw mechanism in order to explain the smallness of neutrino masses, it seems to be difficult, if not impossible, to obtain a nearly degenerate neutrino mass spectrum in a natural way. In order to find natural explanations for partially degenerate neutrino masses, it is therefore promising to consider the type II see-saw mechanism (see e.g. [34, 35, 36, 37]), as has been argued for example in [13, 18].

In this work, we propose a type II upgrade of type I see-saw models leading to new classes of models where partially degenerate neutrinos are as natural as hierarchical ones. This is achieved by a $\text{SO}(3)$ flavour symmetry, which forces the additional type II mass term to be proportional to the unit matrix in leading order. The addition of a type II unit matrix contribution to the type I neutrino mass matrix with a particular phase structure turns out to enable the neutrino mass scale to be increased almost arbitrarily, while leaving the mixing angles approximately unchanged. In this approach the type I

see-saw part of the neutrino mass matrix, which controls the mass squared differences and mixing angles, may be governed by sequential right-handed neutrino dominance and a natural alignment for the SO(3)-breaking vacuum. We focus on classes of models with bi-large mixing originating from the neutrino mass matrix although we also briefly discuss other classes of models where large mixing stems from the charged lepton mass matrix. We also study renormalization group corrections to the mass squared differences and mixings and find that the low energy values do not depend sensitively on the high energy values for partially degenerate neutrinos with a mass scale up to about 0.15 eV. This framework predicts the effective mass for neutrinoless double beta decay to be approximately equal to the neutrino mass scale and therefore neutrinoless double beta decay will be observable if the neutrino mass spectrum is partially degenerate. We also find that all observable CP phases become small as the neutrino mass scale increases.

The layout of the paper is as follows: After giving a motivation in section 2, we outline how naturally small neutrino masses could emerge from type I and type II see-saw mechanisms in section 3. In section 4 we discuss the type II see-saw scenario with spontaneously broken SO(3) flavour symmetry and analyze the consequences for the ingredients of the type II see-saw formula. In section 5 we consider a real alignment mechanism for the SO(3)-breaking vacuum expectation values (vevs) and show how it leads to classes of models where the observed bi-large neutrino mixing can naturally be obtained. In section 6 we focus on models with sequential right-handed neutrino dominance [39, 40] for the type I part of the neutrino mass matrix. We extract the mixing angles, masses and CP phases analytically and discuss the predictions for these parameters from our scenario. In section 7 we study renormalization group corrections to the neutrino mass squared differences and mixings. In section 8 we analyze the predictions for the effective mass for neutrinoless double beta decay. Section 9 contains a discussion and our conclusions.

2 Motivation

For a given mass of the lightest neutrino and e.g. a normal scheme for the neutrino masses $m_1 < m_2 < m_3$, the remaining two masses can be calculated from the requirement that the experimentally measured mass squared differences are produced. Figure 1 shows the neutrino mass eigenvalues as a function of the mass of the lightest neutrino. For a lightest neutrino heavier than about 0.02 eV, the mass eigenvalues of the neutrinos are of the same order. We will refer to the neutrinos as partially degenerate, if the mass of the lightest neutrino is roughly in the range [0.02, 0.15] eV, where m_1 and m_2 are nearly degenerate. This is below what is usually called quasi-degenerate where the masses of all neutrinos are approximately degenerate. This mass range is particularly interesting, since it is not disfavored by unnaturally large radiative corrections and it might be accessible to future $0\nu\beta\beta$ decay searches.

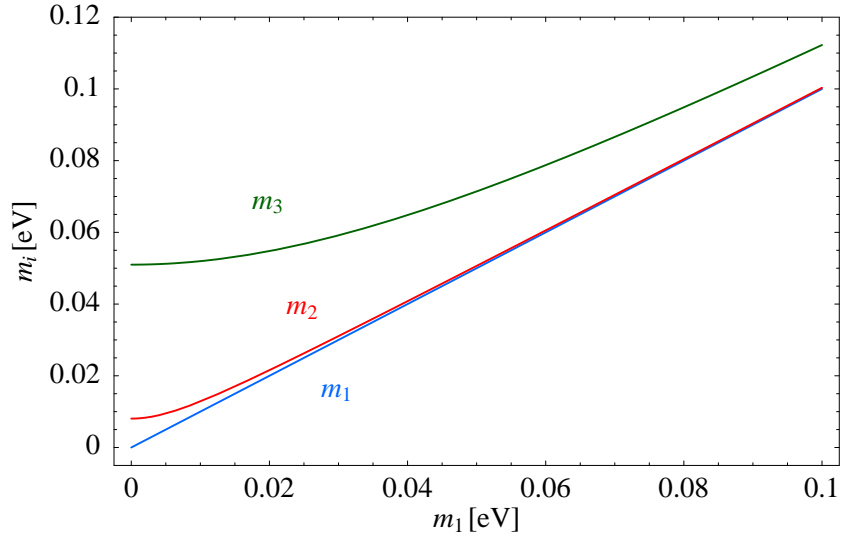


Figure 1: Neutrino masses as a function of the mass of the lightest neutrino in a normal mass scheme, where $m_3 > m_2 > m_1$.

With three left-handed neutrinos contained in the lepton doublets and three right-handed neutrinos which are singlets under $G_{321} := \text{SU}(3)_C \times \text{SU}(2)_L \times \text{U}(1)_Y$, the general neutrino mass matrix is given by

$$\mathcal{L}_{M_\nu} = -\frac{1}{2} \begin{pmatrix} \overline{\nu_L^f} \\ \nu_R^{Ci} \end{pmatrix}^T \begin{pmatrix} (m_{LL}^{\text{II}})_{fg} & (m_{LR})_{fj} \\ (m_{LR}^T)_{ig} & (M_{RR})_{ij} \end{pmatrix} \begin{pmatrix} \nu_L^{Cg} \\ \nu_R^j \end{pmatrix} + \text{h.c.} . \quad (1)$$

Under the assumption that the mass eigenvalues M_{Ri} of M_{RR} are very large compared to the components of m_{LL}^{II} and m_{LR} , the mass matrix can approximately be diagonalized yielding

$$\mathcal{L}_{M_\nu} \approx -\frac{1}{2} \begin{pmatrix} \overline{\nu_L^f} \\ \nu_R^{Ci} \end{pmatrix}^T \begin{pmatrix} (m_{LL}^{\nu})_{fg} & 0 \\ 0 & (M_{RR})_{ij} \end{pmatrix} \begin{pmatrix} \nu_L^{Cg} \\ \nu_R^j \end{pmatrix} + \text{h.c.} , \quad (2)$$

where, neglecting $\mathcal{O}(M_{Ri}^{-1})$ -terms, $\nu_L^f \approx \nu_L^f$ and $\nu_R^{Ci} \approx \nu_R^{Ci}$. The Majorana mass matrix m_{LL}^{ν} for the light left-handed neutrinos is given by

$$m_{LL}^{\nu} \approx m_{LL}^{\text{II}} + m_{LL}^{\text{I}} \quad (3)$$

with

$$m_{LL}^{\text{I}} := -m_{LR} M_{RR}^{-1} m_{LR}^T . \quad (4)$$

The suppression by M_{RR}^{-1} provides a natural explanation for the smallness of neutrino masses from m_{LL}^{I} . This is referred to as the type I see-saw mechanism [9, 10, 11, 12]. As we will sketch in section 3, the direct mass term $m_{\text{LL}}^{\text{II}}$ can also provide a naturally small contribution to the light neutrino masses if it stems e.g. from a see-saw suppressed induced vev. We will refer to the general case, where both possibilities are allowed, as the II see-saw mechanism [34, 35, 36, 37].

In type I see-saw models, it seems to be difficult, if not impossible, to obtain a partially degenerate or quasi-degenerate neutrino mass spectrum in a natural way, whereas hierarchical masses seem to be natural. For a review on neutrino mass models, see e.g. [38]. The direct mass term in type II models on the other hand has the potential to provide a natural way for generating neutrino masses with a partial degeneracy. Imagine for example that by symmetry, the direct mass term is forced to be proportional to the unit matrix in flavour space, $m_{\text{LL}}^{\text{II}} = m^{\text{II}} \mathbb{1}$. We will realize such a direct mass term, which gives a common mass to all the neutrinos, in section 4 via SO(3) flavour symmetry. The type II formula of equation (3) is then realized by

$$m_{\text{LL}}^{\nu} \approx m^{\text{II}} \begin{pmatrix} 1 & 0 & 0 \\ 0 & 1 & 0 \\ 0 & 0 & 1 \end{pmatrix} + \begin{pmatrix} (m_{\text{LL}}^{\text{I}})_{11} & (m_{\text{LL}}^{\text{I}})_{12} & (m_{\text{LL}}^{\text{I}})_{13} \\ (m_{\text{LL}}^{\text{I}})_{21} & (m_{\text{LL}}^{\text{I}})_{22} & (m_{\text{LL}}^{\text{I}})_{23} \\ (m_{\text{LL}}^{\text{I}})_{31} & (m_{\text{LL}}^{\text{I}})_{32} & (m_{\text{LL}}^{\text{I}})_{33} \end{pmatrix} \quad (5)$$

and the direct mass term $m^{\text{II}} \mathbb{1}$ naturally allows for partially degenerate neutrinos. The neutrino mass splittings and mixing angles in this scenario are mainly controlled by the type I see-saw contribution m_{LL}^{I} . To analyze the effect of the type II contribution $m_{\text{LL}}^{\text{II}}$, we consider the diagonalization of m_{LL}^{I} by a unitary transformation $(m_{\text{LL}}^{\text{I}})_{\text{diag}} = V m_{\text{LL}}^{\text{I}} V^T$. If we assume for the moment that the type I see-saw mass matrix m_{LL}^{I} is real, which implies that V is an orthogonal matrix, we obtain

$$(m_{\text{LL}}^{\nu})_{\text{diag}} = m^{\text{II}} V V^T + V m_{\text{LL}}^{\text{I}} V^T = m^{\text{II}} \mathbb{1} + (m_{\text{LL}}^{\text{I}})_{\text{diag}} . \quad (6)$$

The additional direct mass term leaves the predictions for the mixings from the type I see-saw contribution unchanged in this case. This allows to transform many type I see-saw models for hierarchical neutrino masses into type II see-saw models for partially degenerate or quasi-degenerate neutrino masses while maintaining the predictions for the mixing angles. Obviously, in the general complex case, it is no longer that simple since for a unitary matrix $V V^T \neq \mathbb{1}$ and the phases will have impact on the predictions for the mixings. We will return to this issue in section 6 where we will see that e.g. in some classes of models with sequential right-handed neutrino dominance (RHND) [39, 40] for the type I contribution to the neutrino mass matrix, the known techniques and mechanisms for explaining the bi-large lepton mixings can be directly applied also in the presence of CP phases.

Field	\hat{H}_d	\hat{H}_u	$\hat{\Delta}$	$\bar{\hat{\Delta}}$	\hat{L}^f	\hat{e}^{Cf}	$\hat{\nu}^{Cf}$
SU(3) _C	1	1	1	1	1	1	1
SU(2) _L	2	2	3	3	2	1	1
q_Y	$-\frac{1}{2}$	$+\frac{1}{2}$	1	-1	$-\frac{1}{2}$	+1	0

Table 1: Representations under G_{321} of the chiral superfields involved in the generation of lepton masses in the MSSM extended by three singlet superfields which contain the right-handed neutrinos and by two SU(2)_L-triplets.

3 Type I and Type II See-Saw Mechanisms

We now outline how naturally small neutrino masses could emerge from minimal realizations of type I and type II see-saw mechanisms. Let us consider a minimal extension of the MSSM in order to allow for neutrino masses. We discuss the supersymmetric case here since the modifications in order to obtain the non-supersymmetric version are straightforward. Dirac masses for the neutrinos can be achieved by adding chiral superfields $\hat{\nu}^{Ci}$ ($i \in \{1, 2, 3\}$) in the representation $(\mathbf{1}, \mathbf{1}, 0)$ of G_{321} to the particle content, which contain the right-handed neutrinos ν_R^i as fermionic components. If not protected by symmetry, these singlets are expected to obtain large masses M_{Ri} , associated with the scale of lepton number breaking. Lepton masses now arise from the superpotential

$$\mathcal{W}_\ell = -(Y_e)_{gf}(\hat{L}^g \cdot \hat{H}_d) \hat{e}^{Cf} + (Y_\nu)_{fj}(\hat{L}^f \cdot \hat{H}_u) \hat{\nu}^{Cj} + \frac{1}{2} \hat{\nu}^{Ci} (M_{RR})_{ij} \hat{\nu}^{Cj}, \quad (7)$$

where the dot indicates the SU(2)_L invariant product, i.e. $(\hat{L}^j \cdot \hat{H}_u) := \hat{L}_a^j (i\tau_2)^{ab} (\hat{H}_u)_b$ with τ_A ($A \in \{1, 2, 3\}$) being the Pauli matrices. The superfields \hat{H}_u and \hat{H}_d contain the Higgs fields which also give masses to the up-type and down-type quarks respectively. \hat{L} contains the lepton doublets and \hat{e}^C the charged leptons. This yields naturally small neutrino masses by the type I see-saw relation

$$m_{LL}^I = -v_u^2 Y_\nu M_{RR}^{-1} Y_\nu^T. \quad (8)$$

In many cases however, the left-handed neutrinos may also obtain a naturally small direct mass term. This happens for example if SU(2)_L-triplet Higgs superfields $\hat{\Delta}$ and $\bar{\hat{\Delta}}$ are added to the particle spectrum which have weak hypercharge $q_Y = +1$ and $q_Y = -1$, respectively. The representations of the chiral superfields involved in this minimal setup are given in table 1. Only the superfield $\hat{\Delta}$ contributes to the generation of fermion masses via the coupling

$$\mathcal{W}_\Delta = \frac{1}{2} (Y_\Delta^\dagger)_{fg} \hat{L}^{Tf} i\tau_2 \hat{\Delta} \hat{L}^g \quad (9)$$

to the lepton doublets. We have written the $SU(2)_L$ -triplets as traceless 2×2 -matrices

$$\hat{\Delta} = \begin{pmatrix} \hat{\Delta}^+ & \hat{\Delta}^{++} \\ \hat{\Delta}^0 & -\hat{\Delta}^+ \end{pmatrix} \text{ and } \bar{\hat{\Delta}} = \begin{pmatrix} \bar{\hat{\Delta}}^+ & \bar{\hat{\Delta}}^{++} \\ \bar{\hat{\Delta}}^0 & -\bar{\hat{\Delta}}^+ \end{pmatrix}. \quad (10)$$

A vev $v_\Delta = \langle \Delta^0 \rangle$ of the neutral component of the scalar field contained in $\hat{\Delta}$ gives a direct mass for the left-handed neutrinos. We choose v_Δ to be real and positive by a proper phase choice for $\hat{\Delta}$. In order to estimate the natural size of v_Δ , we consider the Higgs potential from the part

$$\mathcal{W}_H = M_\Delta \text{Tr}(\hat{\Delta} \bar{\hat{\Delta}}) + \lambda_u \hat{H}_u^T i\tau_2 \bar{\hat{\Delta}} \hat{H}_u + \lambda_d \hat{H}_d^T i\tau_2 \hat{\Delta} \hat{H}_d + \mu (\hat{H}_d \cdot \hat{H}_u) \quad (11)$$

of the superpotential. Using the expansion of the superfields $\hat{H}_u = H_u + \sqrt{2}\theta\tilde{H}_u + \theta\theta F_{H_u}$ and $\hat{\Delta} = \Delta + \sqrt{2}\theta\tilde{\Delta} + \theta\theta F_\Delta$, we see that the scalar potential from $|F_\Delta|^2$ contains the terms

$$\mathcal{V} = M_\Delta \lambda_u H_u^T i\tau_2 \Delta^* H_u + M_\Delta^2 \text{Tr}(\Delta^* \Delta) + \text{h.c.} . \quad (12)$$

After EW symmetry breaking, this results in a tadpole which forces Δ to get an induced vev of the order

$$v_\Delta \approx \frac{\lambda_u v_u^2}{M_\Delta}. \quad (13)$$

Analogously, the neutral component of the superfield $\bar{\hat{\Delta}}$ obtains a small vev as well, however it is not relevant here since $\bar{\hat{\Delta}}$ does not couple to the fermions. If M_Δ is large, say of the order of one of the eigenvalues of M_{RR} , this leads to another naturally small contribution

$$m_{\text{LL}}^{\text{II}} = Y_\Delta v_\Delta \quad (14)$$

to the neutrino mass matrix, which is now given by the type II see-saw formula

$$m_{\text{LL}}^\nu = m_{\text{LL}}^{\text{II}} + m_{\text{LL}}^{\text{I}} = Y_\Delta v_\Delta - v_u^2 Y_\nu M_{\text{RR}}^{-1} Y_\nu^T. \quad (15)$$

The contributions to neutrino masses in the considered minimal type II scenario are illustrated in figure 2. Note that we do not require left-right symmetry throughout this paper. Additional triplets like the ones used here to provide a minimal example for a type II see-saw mechanism typically appear in models with a left-right symmetric particle content like minimal left-right symmetric models [41, 42, 43], Pati-Salam models [44] or $SO(10)$ -GUTs [45, 46]. However, a naturally small direct vev can also originate from other sources like e.g. from higher-dimensional operators and most of the results of this paper can also be applied to this case.

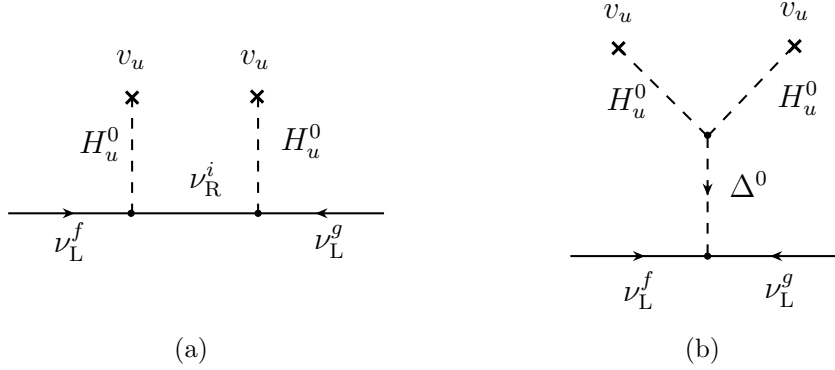


Figure 2: Diagrams leading to neutrino masses in the type II see-saw scenario. Diagram (a) shows the contribution from the exchange of a heavy right-handed neutrino as in the type I see-saw mechanism. Diagram (b) illustrates the contribution from an induced vev of the triplet Δ . At low energy, they can be viewed as contributions to the effective neutrino mass operator from integrating out the heavy fields ν_R^i and Δ^0 , respectively.

4 Type II See-Saw with SO(3) Flavour Symmetry

We now show how a contribution to the neutrino mass matrix proportional to the unit matrix can be achieved by a spontaneously broken SO(3) flavour symmetry. We will analyze the consequences of such a framework for the masses and mixings in the lepton sector, where we consider the case that SO(3) acts on the lepton doublets. This has impact on the ingredients of the type II see-saw formula for the neutrino mass matrix of equation (15) as well as for the mass matrix of the charged leptons.

4.1 Structure of the Ingredients of the Type II See-Saw

In order to break SO(3) spontaneously, we introduce additional heavy G_{321} -singlet superfields $\hat{\theta}_I$ ($I \in \{1, 2, 3\}$) which are flavour triplets and acquire vevs $\langle\langle \theta_I \rangle\rangle_f$. In order to associate each flavon field $\hat{\theta}_I$ with one of the right-handed neutrino superfields $\hat{\nu}^{Ci}$, we introduce three discrete symmetries Z_2^I . The representations of the fields involved in the generation of the neutrino mass matrix are given in table 2.

The renormalizable term for neutrino Yukawa couplings is forbidden by the SO(3) flavour symmetry. Dirac masses for the neutrinos can however be generated by the higher-dimensional operators

$$\begin{aligned}
 \mathcal{W}_{Y_\nu} = & a_1 (\hat{L}^f \cdot \hat{H}_u) \hat{\nu}^{C1} \frac{\langle\langle \theta_1 \rangle\rangle_f}{M_{N1}} + a_2 (\hat{L}^f \cdot \hat{H}_u) \hat{\nu}^{C2} \frac{\langle\langle \theta_2 \rangle\rangle_f}{M_{N2}} \\
 & + a_3 (\hat{L}^f \cdot \hat{H}_u) \hat{\nu}^{C3} \frac{\langle\langle \theta_3 \rangle\rangle_f}{M_{N3}} + \dots
 \end{aligned} \tag{16}$$

Field	\hat{L}	$\hat{\Delta}$	\hat{H}_u	$\hat{\nu}^{C1}$	$\hat{\nu}^{C2}$	$\hat{\nu}^{C3}$	$\hat{\theta}_1$	$\hat{\theta}_2$	$\hat{\theta}_3$
SO(3)	3	1	1	1	1	1	3	3	3
Z_2^1	+	+	+	-	+	+	-	+	+
Z_2^2	+	+	+	+	-	+	+	-	+
Z_2^3	+	+	+	+	+	-	+	+	-

Table 2: Representations of $\text{SO}(3) \times (Z_2)^3$ involved in the generation of neutrino masses.

M_{NI} correspond to the masses of some Froggatt-Nielsen fields [47] which are integrated out and produce the effective operators. In leading order the neutrino Yukawa matrix is thus given by

$$Y_\nu^0 = \begin{pmatrix} a_1 \frac{\langle(\theta_1)_1\rangle}{M_{N1}} & a_2 \frac{\langle(\theta_2)_1\rangle}{M_{N2}} & a_3 \frac{\langle(\theta_3)_1\rangle}{M_{N3}} \\ a_1 \frac{\langle(\theta_1)_2\rangle}{M_{N1}} & a_2 \frac{\langle(\theta_2)_2\rangle}{M_{N2}} & a_3 \frac{\langle(\theta_3)_2\rangle}{M_{N3}} \\ a_1 \frac{\langle(\theta_1)_3\rangle}{M_{N1}} & a_2 \frac{\langle(\theta_2)_3\rangle}{M_{N2}} & a_3 \frac{\langle(\theta_3)_3\rangle}{M_{N3}} \end{pmatrix}. \quad (17)$$

The Majorana mass term for the right-handed neutrinos is restricted by the discrete symmetries and for our choice of Z_2 symmetries given by

$$\begin{aligned} \mathcal{W}_{M_{RR}} &= \frac{1}{2} \hat{\nu}^{C1} M_{R1} \hat{\nu}^{C1} + \frac{1}{2} \hat{\nu}^{C2} M_{R2} \hat{\nu}^{C2} + \frac{1}{2} \hat{\nu}^{C3} M_{R3} \hat{\nu}^{C3} \\ &+ \frac{1}{2} \sum_{i,j,I,J=1}^3 \hat{\nu}^{Ci} (M'_{RR})_{ij} \hat{\nu}^{Cj} \delta_{iI} \delta_{jJ} \sum_{f=1}^3 \frac{\langle(\theta_I)_f\rangle \langle(\theta_J)_f\rangle}{M_{N'I} M_{N'J}} + \dots \end{aligned} \quad (18)$$

At leading order, the mass matrix is thus forced to a diagonal structure

$$M_{RR}^0 = \begin{pmatrix} M_{R1} & 0 & 0 \\ 0 & M_{R2} & 0 \\ 0 & 0 & M_{R3} \end{pmatrix}. \quad (19)$$

In the presence of the $\text{SO}(3)$ symmetry, the couplings of the lepton doublets to the triplet Higgs superfield $\hat{\Delta}$ are given by

$$\mathcal{W}_\Delta = y_\Delta \hat{L}^{Tf} i\tau_2 \hat{\Delta} \hat{L}^f + \sum_{f,g=1}^3 \hat{L}^{Tf} i\tau_2 \hat{\Delta} \hat{L}^g \sum_{I=1}^3 b_I \frac{\langle(\theta_I)_f\rangle \langle(\theta_I)_g\rangle}{M_{LI}^2} + \dots \quad (20)$$

At leading order, this results in a contribution $Y_\Delta v_\Delta$ to the neutrino mass matrix proportional to the unit matrix in flavour space,

$$Y_\Delta^0 = y_\Delta \begin{pmatrix} 1 & 0 & 0 \\ 0 & 1 & 0 \\ 0 & 0 & 1 \end{pmatrix}. \quad (21)$$

Assuming $M_{NI} = M_{N'I} = M_{LI}$, the next-to-leading order operators are of the order $(\langle(\theta_I)_f\rangle/M_{NI})^2 \approx (Y_\nu^0)_{If}^2$. If the neutrino Yukawa couplings are very small, the next-to-leading order operators are strongly suppressed and can approximately be neglected. However, if the effective field theory expansion parameters $\langle(\theta_I)_f\rangle/M_{NI}$ are relatively large, we should stress that a careful analysis of higher-dimensional operators of the superpotential and also of the Kähler potential (see e.g. [48]) has to be performed. Let us consider for example the effect of a neutrino Yukawa coupling $(Y_\nu^0)_{33} \approx \langle(\theta_3)_3\rangle/M_{N3} \approx 0.1$. The next-to-leading order operators of equation (20) induce a contribution to the atmospheric mass squared difference $\Delta m_{\text{atm}}^2 := m_3^2 - m_1^2$ for a given scale of the direct mass term $m^{\text{II}} \mathbb{1} = y_\Delta v_\Delta \mathbb{1}$. If we take for example $m^{\text{II}} \approx 0.1$ eV and set $b_3 = y_\Delta$ and $a_3 = 1$ for simplicity, this would induce a contribution to Δm_{atm}^2 of about $2 \cdot 10^{-4}$ eV², which is still about an order of magnitude below the observed experimental value and thus provides only a rather small correction. Since we will not assume particularly large neutrino Yukawa couplings in this work, we will ignore the next-to-leading order operators in the following.

4.2 The Mass Matrix of the Charged Leptons

Before we turn to classes of models which illustrate the mechanism, we discuss the generation of the mass matrix for the charged leptons. The most unrestricted case can be achieved by introducing three new additional flavour-triplet Higgs superfields $(\hat{\chi}_I)_f$ and three additional Z'_2 symmetries, as specified in table 3. This results in a general

Field	\hat{e}^{C1}	\hat{e}^{C2}	\hat{e}^{C3}	$\hat{\chi}_1$	$\hat{\chi}_2$	$\hat{\chi}_3$
SO(3)	1	1	1	3	3	3
Z_2^1	-	+	+	-	+	+
Z_2^2	+	-	+	+	-	+
Z_2^3	+	+	-	+	+	-

Table 3: Representations of the charged leptons and new G_{321} -singlets under the horizontal symmetries $\text{SO}(3) \times (Z'_2)^3$, leading to the most unrestricted scenario. The fields are singlets under the symmetries Z_2^1, Z_2^2 and Z_2^3 .

charged lepton Yukawa matrix generated by higher-dimensional operators, which can be hierarchical from a hierarchy of the vevs $\langle(\chi_1)_f\rangle$, $\langle(\chi_2)_f\rangle$ and $\langle(\chi_3)_f\rangle$ or from the masses of the Froggatt-Nielsen fields. The superpotential operators for the Yukawa interactions are

$$\begin{aligned} \mathcal{W}_{Y_e} = & -a'_1 (\hat{L}^f \cdot \hat{H}_d) \hat{e}^{C1} \frac{\langle(\chi_1)_f\rangle}{M_{E1}} - a'_2 (\hat{L}^f \cdot \hat{H}_d) \hat{e}^{C2} \frac{\langle(\chi_2)_f\rangle}{M_{E2}} \\ & - a'_3 (\hat{L}^f \cdot \hat{H}_d) \hat{e}^{C3} \frac{\langle(\chi_3)_f\rangle}{M_{E3}} - \dots \end{aligned} \quad (22)$$

The $\mathcal{O}(1)$ -coefficients a_1, a_2, a_3 and a'_1, a'_2, a'_3 stem from the realization of the effective operators and are in principle calculable within an underlying full theory. The leading order Yukawa matrix for the charged leptons is given by

$$Y_e^0 = \begin{pmatrix} a'_1 \frac{\langle(\chi_1)_1\rangle}{M_{E1}} & a'_2 \frac{\langle(\chi_2)_1\rangle}{M_{E2}} & a'_3 \frac{\langle(\chi_3)_1\rangle}{M_{E3}} \\ a'_1 \frac{\langle(\chi_1)_2\rangle}{M_{E1}} & a'_2 \frac{\langle(\chi_2)_2\rangle}{M_{E2}} & a'_3 \frac{\langle(\chi_3)_2\rangle}{M_{E3}} \\ a'_1 \frac{\langle(\chi_1)_3\rangle}{M_{E1}} & a'_2 \frac{\langle(\chi_2)_3\rangle}{M_{E2}} & a'_3 \frac{\langle(\chi_3)_3\rangle}{M_{E3}} \end{pmatrix}. \quad (23)$$

Different choices of discrete symmetries and flavon fields involved in the generation of the charged lepton mass matrix can give more predictive scenarios. Obviously, the $\text{SO}(3)$ symmetry might leave the quark sector completely unaffected. On the other hand, the framework discussed so far can also be extended to the quark sector, yielding rather unrestricted quark masses with a natural hierarchy among the columns of the quark Yukawa matrices. For the present however, and in the rest of the paper, we restrict ourselves to the lepton sector.

5 $\text{SO}(3)$ Vacuum Alignment

To stay as minimal as possible, we consider in the following the case that the charged leptons couple to the the same flavon fields $\hat{\theta}_I$ as the neutrinos. This corresponds to replacing $Z_2^I \rightarrow Z_2^I$ and $(\hat{\chi}_I)_f \rightarrow (\hat{\theta}_I)_f$ in section 4.2. The Yukawa matrix of the charged leptons is then related to the neutrino Yukawa matrix. The $\text{SO}(3)$ flavour symmetry in the lepton sector is spontaneously broken by the vevs $\langle(\theta_1)_f\rangle$. Let us consider first the general case with complex vevs. A simultaneous $\text{SO}(3)$ rotation of the three vevs allows to eliminate three real degrees of freedom. We will shortly consider a scenario where the $\text{SO}(3)$ vacuum is aligned such that the vevs are real. Complex phases in the Yukawa matrices Y_ν and Y_e then stem entirely from the coefficients a_1, a_2, a_3 and a'_1, a'_2, a'_3 . It turns out that with this vacuum alignment, which allows for three texture zeros in the Yukawa matrices, the type II scenario can realize the observed masses and mixings in the lepton sector in a particularly natural way.

5.1 Real Alignment for the SO(3) Vacuum

A possibility to achieve real vevs is to introduce three driving superfields \hat{A} , \hat{B} and \hat{C} and to assume a superpotential of the form

$$\mathcal{W} = \hat{A}(\hat{\theta}_1^2 - \Lambda_1^2) + \hat{B}(\hat{\theta}_2^2 - \Lambda_2^2) + \hat{C}(\hat{\theta}_3^2 - \Lambda_3^2) \quad (24)$$

with positive soft mass squareds

$$m_{\theta_1}^2 > 0, \quad m_{\theta_2}^2 > 0 \quad \text{and} \quad m_{\theta_3}^2 > 0 \quad (25)$$

for the scalar components θ_1, θ_2 and θ_3 of the flavon superfields $\hat{\theta}_1, \hat{\theta}_2$ and $\hat{\theta}_3$ (see e.g. [27]). Λ_1, Λ_2 and Λ_3 could stem from vevs of some SO(3)-singlets. They can be chosen positive and real by a proper phase choice for these fields. Let us explicitly consider the vacuum alignment for θ_1 . Minimization of $|F_A|^2$ yields

$$\Lambda_1^2 = \sum_f (\text{Re} \langle (\theta_1)_f \rangle)^2 - \sum_i (\text{Im} \langle (\theta_1)_f \rangle)^2 + 2i \sum_f \text{Re} \langle (\theta_1)_f \rangle \text{Im} \langle (\theta_1)_f \rangle. \quad (26)$$

With our choice $\Lambda_1 \in \mathbb{R}^+$, this leads to the two conditions

$$0 = \sum_f \text{Re} \langle (\theta_1)_f \rangle \text{Im} \langle (\theta_1)_f \rangle, \quad (27a)$$

$$\Lambda_1^2 = \sum_f (\text{Re} \langle (\theta_1)_f \rangle)^2 - \sum_f (\text{Im} \langle (\theta_1)_f \rangle)^2. \quad (27b)$$

The soft mass term $\mathcal{V}_s = m_{\theta_1}^2 \theta_1^* \theta_1$ deforms the driving potential and its minimization under the conditions from $|F_A|^2$ results in $\text{Im} \langle (\theta_1)_f \rangle = 0$ for all components $f \in \{1, 2, 3\}$. This can be seen by plugging equation (27b) into \mathcal{V}_s , which yields

$$\begin{aligned} \mathcal{V}_s &= m_{\theta_1}^2 \left[\sum_f (\text{Re} \langle (\theta_1)_f \rangle)^2 + \sum_f (\text{Im} \langle (\theta_1)_f \rangle)^2 \right] \\ &= m_{\theta_1}^2 \left[\Lambda_1^2 + 2 \sum_f (\text{Im} \langle (\theta_1)_f \rangle)^2 \right]. \end{aligned} \quad (28)$$

Thus, the small positive mass squared forces the vev $\langle \theta_1 \rangle$ to be real. Treating $\langle \theta_2 \rangle$ and $\langle \theta_3 \rangle$ analogously, we obtain a real alignment for the vevs of all scalar components of the flavon superfields,

$$\text{Im} \langle \theta_1 \rangle = 0, \quad \text{Im} \langle \theta_2 \rangle = 0, \quad \text{Im} \langle \theta_3 \rangle = 0. \quad (29)$$

The moduli of the vev vectors are given by

$$|\langle \theta_1 \rangle|^2 \approx \Lambda_1^2, \quad |\langle \theta_2 \rangle|^2 \approx \Lambda_2^2, \quad |\langle \theta_3 \rangle|^2 \approx \Lambda_3^2, \quad (30)$$

which could lead to a hierarchy among the vevs via a hierarchy among Λ_1 , Λ_2 and Λ_3 .

We can now use the $\text{SO}(3)$ freedom to set two components of one of the vev vectors, say $\langle(\theta_I)_f\rangle$, and one corresponding component of a second vev vector, say $\langle(\theta_J)_f\rangle$, to zero. Defining the real expansion parameters

$$\varepsilon_I := |a_I| \frac{\Lambda_I}{M_{NI}}, \quad \varepsilon_J := |a_J| \frac{\Lambda_J}{M_{NJ}}, \quad \varepsilon_K := |a_K| \frac{\Lambda_K}{M_{NK}}, \quad (31a)$$

$$\varepsilon'_I := |a'_I| \frac{\Lambda_I}{M_{EI}}, \quad \varepsilon'_J := |a'_J| \frac{\Lambda_J}{M_{EJ}}, \quad \varepsilon'_K := |a'_K| \frac{\Lambda_K}{M_{EK}}, \quad (31b)$$

without loss of generality we can write

$$a_I \frac{\langle\theta_I\rangle}{M_{NI}} := \begin{pmatrix} 0 \\ 0 \\ h e^{i\delta_I} \varepsilon_I \end{pmatrix}, \quad a_J \frac{\langle\theta_J\rangle}{M_{NJ}} := \begin{pmatrix} 0 \\ e e^{i\delta_J} \varepsilon_J \\ f e^{i\delta_J} \varepsilon_J \end{pmatrix}, \quad a_K \frac{\langle\theta_K\rangle}{M_{NK}} := \begin{pmatrix} a e^{i\delta_K} \varepsilon_K \\ b e^{i\delta_K} \varepsilon_K \\ c e^{i\delta_K} \varepsilon_K \end{pmatrix}, \quad (32a)$$

$$a'_I \frac{\langle\theta_I\rangle}{M_{EI}} := \begin{pmatrix} 0 \\ 0 \\ h e^{i\delta'_I} \varepsilon'_I \end{pmatrix}, \quad a'_J \frac{\langle\theta_J\rangle}{M_{EJ}} := \begin{pmatrix} 0 \\ e e^{i\delta'_J} \varepsilon'_J \\ f e^{i\delta'_J} \varepsilon'_J \end{pmatrix}, \quad a'_K \frac{\langle\theta_K\rangle}{M_{EK}} := \begin{pmatrix} a e^{i\delta'_K} \varepsilon'_K \\ b e^{i\delta'_K} \varepsilon'_K \\ c e^{i\delta'_K} \varepsilon'_K \end{pmatrix}, \quad (32b)$$

with real coefficients $\{a, b, c, e, f, h\}$ satisfying

$$h \approx 1, \quad e^2 + f^2 \approx 1, \quad a^2 + b^2 + c^2 \approx 1. \quad (33)$$

We choose the convention that the labels $\{1, 2, 3\}$ are assigned to I, J and K such that

$$\varepsilon'_3 > \varepsilon'_2 > \varepsilon'_1 \quad (34)$$

holds in the charged lepton sector. This also defines the labels of $\varepsilon_1, \varepsilon_2$ and ε_3 and of the heavy mass eigenvalues M_{R1}, M_{R2} and M_{R3} of the right-handed neutrinos. In the following, by a global phase transformation of all the leptons, we arrange for the direct mass term for the neutrinos proportional to the unit matrix to be real and positive. In addition, we absorb possible phases of M_{R1}, M_{R2} and M_{R3} in the columns of Y_ν . The phases in the Yukawa matrices then stem from the coefficients a_1, a_2, a_3 and a'_1, a'_2, a'_3 which are in general complex,

$$\delta_1 := \text{Arg}(a_1), \quad \delta_2 := \text{Arg}(a_2), \quad \delta_3 := \text{Arg}(a_3), \quad (35a)$$

$$\delta'_1 := \text{Arg}(a'_1), \quad \delta'_2 := \text{Arg}(a'_2), \quad \delta'_3 := \text{Arg}(a'_3). \quad (35b)$$

5.2 Textures for the Yukawa Matrices and Type II Scenarios

The parameterization of the the $\text{SO}(3)$ -breaking vacuum specified in equation (32) uses the basis where the Yukawa matrices Y_ν and Y_e each have three zero entries. Motivation for this choice of basis would come from a full theory beyond the framework presented here. Table 4 shows the textures for Y_ν and Y_e for different proportions of $\varepsilon'_I, \varepsilon'_J$ and

ε'_K using the ordering convention $\varepsilon'_3 > \varepsilon'_2 > \varepsilon'_1$. Additional characteristic features of the Yukawa matrices are that each column has a common complex phase and that, without additional symmetries, the non-zero components of each column have a common typical order of magnitude defined by the expansion parameters $\varepsilon_1, \varepsilon_2, \varepsilon_3$ and $\varepsilon'_1, \varepsilon'_2, \varepsilon'_3$. The hierarchy among the masses of the charged leptons can naturally be realized via $\varepsilon'_3 \gg \varepsilon'_2 \gg \varepsilon'_1$, which we will assume in the following.

5.2.1 Models Type A: Large Mixing θ_{23} from the Neutrino Mass Matrix

In the models of type A, the mixing θ_{23}^e from the charged lepton mass matrix M_e is approximately zero. The almost maximal total lepton mixing θ_{23} thus has to be generated in the neutrino mass matrix. This can for example be achieved if the dominant contribution to the type I part of the neutrino mass matrix stems from the right-handed neutrino ν_R^2 for model A1 or ν_R^1 for model A2. As in the single right handed neutrino dominance case [49, 50] for a pure type I neutrino mass matrix, the condition for a nearly maximal θ_{23} is $|e| \approx |f|$. In addition, the zero in the first element of the column containing the coefficients e and f in general avoids the generation of a large θ_{13}^ν from the neutrino mass matrix. Model A1 has the additional feature that θ_{12}^e and θ_{13}^e are very small, whereas in model type A2 a charged lepton mixing $\tan(\theta_{12}^e) = a/b$ is generated which induces a contribution to the total lepton mixings θ_{12} and θ_{13} . In order not to violate the CHOOZ bound on θ_{13} , θ_{12}^e has to be rather small which means that a has to be somewhat smaller than b . Consequently, the large mixing $\theta_{12} \approx 32^\circ$ should be generated mainly in the neutrino sector. With sequential right-handed neutrino dominance [39, 40] for m_{LL}^1 , this can easily be realized. We will study model A1 in detail in section 6.

5.2.2 Models Type B: Large Mixing θ_{23} from the Charged Leptons

The mixing θ_{23}^e from the charge lepton mass matrix is given by $\tan(\theta_{23}^e) \approx e/f$. $e \approx f$ can explain the nearly maximal total lepton mixing θ_{23} in a lopsided mass model, provided that the contribution θ_{23}^ν is small, which can e.g. be achieved if ν_R^2 is the dominant right-handed neutrino for model B1 and ν_R^1 for model B2. Since as for the model A2, a large θ_{12}^e in model B2 would induce a large contribution to θ_{13} , the large solar mixing should be generated by the neutrino mass matrix.

5.2.3 Models Type C: Large Angles for all the Charged Lepton Mixings

For models of type C, it is possible to generate bi-large lepton mixing entirely from Y_e . Small mixing from the neutrino mass matrix would correspond to ν_R^1 being the dominant right-handed neutrino and ν_R^2 being subdominant for model C1 or to ν_R^1 being dominant and ν_R^2 being subdominant for model C2. For the model C2, the large mixings are given by $\tan(\theta_{12}) = a/b$ and $\tan(\theta_{23}) = \sqrt{a^2 + b^2}/c$ (see also [51]). While $\theta_{13} \approx 0$ for model C2, it has to be taken care that θ_{13} is below the experimental bounds in model C1.

Model	Y_ν^0	Y_e^0
A1	$\begin{pmatrix} a e^{i\delta_1} \varepsilon_1 & 0 & 0 \\ b e^{i\delta_1} \varepsilon_1 & e e^{i\delta_2} \varepsilon_2 & 0 \\ c e^{i\delta_1} \varepsilon_1 & f e^{i\delta_2} \varepsilon_2 & h e^{i\delta_3} \varepsilon_3 \end{pmatrix}$	$\begin{pmatrix} a e^{i\delta'_1} \varepsilon'_1 & 0 & 0 \\ b e^{i\delta'_1} \varepsilon'_1 & e e^{i\delta'_2} \varepsilon'_2 & 0 \\ c e^{i\delta'_1} \varepsilon'_1 & f e^{i\delta'_2} \varepsilon'_2 & h e^{i\delta'_3} \varepsilon'_3 \end{pmatrix}$
A2	$\begin{pmatrix} 0 & a e^{i\delta_2} \varepsilon_2 & 0 \\ e e^{i\delta_1} \varepsilon_1 & b e^{i\delta_2} \varepsilon_2 & 0 \\ f e^{i\delta_1} \varepsilon_1 & c e^{i\delta_2} \varepsilon_2 & h e^{i\delta_3} \varepsilon_3 \end{pmatrix}$	$\begin{pmatrix} 0 & a e^{i\delta'_2} \varepsilon'_2 & 0 \\ e e^{i\delta'_1} \varepsilon'_1 & b e^{i\delta'_2} \varepsilon'_2 & 0 \\ f e^{i\delta'_1} \varepsilon'_1 & c e^{i\delta'_2} \varepsilon'_2 & h e^{i\delta'_3} \varepsilon'_3 \end{pmatrix}$
B1	$\begin{pmatrix} a e^{i\delta_1} \varepsilon_1 & 0 & 0 \\ b e^{i\delta_1} \varepsilon_1 & 0 & e e^{i\delta_3} \varepsilon_3 \\ c e^{i\delta_1} \varepsilon_1 & h e^{i\delta_2} \varepsilon_2 & f e^{i\delta_3} \varepsilon_3 \end{pmatrix}$	$\begin{pmatrix} a e^{i\delta'_1} \varepsilon'_1 & 0 & 0 \\ b e^{i\delta'_1} \varepsilon'_1 & 0 & e e^{i\delta'_3} \varepsilon'_3 \\ c e^{i\delta'_1} \varepsilon'_1 & h e^{i\delta'_2} \varepsilon'_2 & f e^{i\delta'_3} \varepsilon'_3 \end{pmatrix}$
B2	$\begin{pmatrix} 0 & a e^{i\delta_2} \varepsilon_2 & 0 \\ 0 & b e^{i\delta_2} \varepsilon_2 & e e^{i\delta_3} \varepsilon_3 \\ h e^{i\delta_1} \varepsilon_1 & c e^{i\delta_2} \varepsilon_2 & f e^{i\delta_3} \varepsilon_3 \end{pmatrix}$	$\begin{pmatrix} 0 & a e^{i\delta'_2} \varepsilon'_2 & 0 \\ 0 & b e^{i\delta'_2} \varepsilon'_2 & e e^{i\delta'_3} \varepsilon'_3 \\ h e^{i\delta'_1} \varepsilon'_1 & c e^{i\delta'_2} \varepsilon'_2 & f e^{i\delta'_3} \varepsilon'_3 \end{pmatrix}$
C1	$\begin{pmatrix} 0 & 0 & a e^{i\delta_3} \varepsilon_3 \\ 0 & e e^{i\delta_2} \varepsilon_2 & b e^{i\delta_3} \varepsilon_3 \\ h e^{i\delta_1} \varepsilon_1 & f e^{i\delta_2} \varepsilon_2 & c e^{i\delta_3} \varepsilon_3 \end{pmatrix}$	$\begin{pmatrix} 0 & 0 & a e^{i\delta'_3} \varepsilon'_3 \\ 0 & e e^{i\delta'_2} \varepsilon'_2 & b e^{i\delta'_3} \varepsilon'_3 \\ h e^{i\delta'_1} \varepsilon'_1 & f e^{i\delta'_2} \varepsilon'_2 & c e^{i\delta'_3} \varepsilon'_3 \end{pmatrix}$
C2	$\begin{pmatrix} 0 & 0 & a e^{i\delta_3} \varepsilon_3 \\ e e^{i\delta_1} \varepsilon_1 & 0 & b e^{i\delta_3} \varepsilon_3 \\ f e^{i\delta_1} \varepsilon_1 & h e^{i\delta_2} \varepsilon_2 & c e^{i\delta_3} \varepsilon_3 \end{pmatrix}$	$\begin{pmatrix} 0 & 0 & a e^{i\delta'_3} \varepsilon'_3 \\ e e^{i\delta'_1} \varepsilon'_1 & 0 & b e^{i\delta'_3} \varepsilon'_3 \\ f e^{i\delta'_1} \varepsilon'_1 & h e^{i\delta'_2} \varepsilon'_2 & c e^{i\delta'_3} \varepsilon'_3 \end{pmatrix}$

Table 4: Textures for the leading order Yukawa matrices from real vacuum alignment with three zero entries. The motivation for choosing such a basis would come a full theory beyond the scope of the framework presented here. We use the convention that the right-handed lepton fields multiply the Yukawa matrices from the right, as defined in equation (16) and (22). Our sorting of the vev vectors and labeling of the columns of Y_ν^0 and Y_e^0 is such that $\varepsilon'_3 > \varepsilon'_2 > \varepsilon'_1$. The mass matrix M_{RR}^0 of the right-handed neutrinos is diagonal (see equation (18)) and the direct mass term for the neutrinos is given by $m^{\text{II}} \mathbb{1}$ at leading order. This leads to type II see-saw models with either small mixing from the charged leptons and bi-large mixing from the neutrinos (A1 and A2), large atmospheric mixing from the charged leptons (B1 and B2) or models where in principle all mixing can be produced via the charged lepton mass matrix (C1 and C2). The neutrino mass squared differences and the contributions to the lepton mixings from the type I neutrino mass matrix depend crucially on the ratios $\varepsilon_1^2/M_{\text{R1}}, \varepsilon_2^2/M_{\text{R2}}, \varepsilon_3^2/M_{\text{R3}}$. The hierarchy among the masses of the charged leptons can naturally be realized via a hierarchy $\varepsilon'_3 \gg \varepsilon'_2 \gg \varepsilon'_1$.

6 A Type II Scenario with Sequential RHND

As an example for a type II model where the bi-large lepton mixing stems from the neutrino mass matrix, we now consider explicitly the model A1 of table 4. We make the additional assumption of sequential righthanded neutrino dominance (RHND) [39, 40], leading to a hierarchical type I part m_ν^I of the neutrino mass matrix. The vev structure for this case allows to define (see equation (32))

$$a_3 \frac{\langle \theta_3 \rangle}{M_{N3}} := \begin{pmatrix} 0 \\ 0 \\ h e^{i\delta_3} \varepsilon_3 \end{pmatrix}, \quad a_2 \frac{\langle \theta_2 \rangle}{M_{N2}} := \begin{pmatrix} 0 \\ e e^{i\delta_2} \varepsilon_2 \\ f e^{i\delta_2} \varepsilon_2 \end{pmatrix}, \quad a_1 \frac{\langle \theta_1 \rangle}{M_{N1}} := \begin{pmatrix} a e^{i\delta_1} \varepsilon_1 \\ b e^{i\delta_1} \varepsilon_1 \\ c e^{i\delta_1} \varepsilon_1 \end{pmatrix}, \quad (36a)$$

$$a'_3 \frac{\langle \theta_3 \rangle}{M_{E3}} := \begin{pmatrix} 0 \\ 0 \\ h e^{i\delta'_3} \varepsilon'_3 \end{pmatrix}, \quad a'_2 \frac{\langle \theta_2 \rangle}{M_{E2}} := \begin{pmatrix} 0 \\ e e^{i\delta'_2} \varepsilon'_2 \\ f e^{i\delta'_2} \varepsilon'_2 \end{pmatrix}, \quad a'_1 \frac{\langle \theta_1 \rangle}{M_{E1}} := \begin{pmatrix} a e^{i\delta'_1} \varepsilon'_1 \\ b e^{i\delta'_1} \varepsilon'_1 \\ c e^{i\delta'_1} \varepsilon'_1 \end{pmatrix}, \quad (36b)$$

leading to the Yukawa matrices

$$Y_\nu^0 = \begin{pmatrix} a e^{i\delta_1} \varepsilon_1 & 0 & 0 \\ b e^{i\delta_1} \varepsilon_1 & e e^{i\delta_2} \varepsilon_2 & 0 \\ c e^{i\delta_1} \varepsilon_1 & f e^{i\delta_2} \varepsilon_2 & h e^{i\delta_3} \varepsilon_3 \end{pmatrix}, \quad Y_e^0 = \begin{pmatrix} a e^{i\delta'_1} \varepsilon'_1 & 0 & 0 \\ b e^{i\delta'_1} \varepsilon'_1 & e e^{i\delta'_2} \varepsilon'_2 & 0 \\ c e^{i\delta'_1} \varepsilon'_1 & f e^{i\delta'_2} \varepsilon'_2 & h e^{i\delta'_3} \varepsilon'_3 \end{pmatrix}. \quad (37)$$

In order to match notation with reference [39, 40], we define

$$M_{\text{RR}}^0 =: \begin{pmatrix} X & 0 & 0 \\ 0 & Y & 0 \\ 0 & 0 & X' \end{pmatrix}, \quad (38)$$

denoting the mass of the dominant right-handed neutrino by Y and the mass of the subdominant one by X . The sequential RHND condition we impose is then

$$\left| \frac{\varepsilon_2^2}{Y} \right| \gg \left| \frac{\varepsilon_1^2}{X} \right| \gg \left| \frac{\varepsilon_3^2}{X'} \right|. \quad (39)$$

The leading order type II neutrino mass matrix is then given by

$$m_{\text{LL}}^\nu = m^{\text{II}} \begin{pmatrix} 1 & 0 & 0 \\ 0 & 1 & 0 \\ 0 & 0 & 1 \end{pmatrix} - \frac{e^{i2\delta_2} \varepsilon_2^2 v_u^2}{Y} \begin{pmatrix} 0 & 0 & 0 \\ 0 & e^2 & ef \\ 0 & ef & f^2 \end{pmatrix} - \frac{e^{i2\delta_1} \varepsilon_1^2 v_u^2}{X} \begin{pmatrix} a^2 & ab & ac \\ ab & b^2 & bc \\ ac & bc & c^2 \end{pmatrix}. \quad (40)$$

We now analyze the lepton masses, mixings and CP phases which are generated by m_{LL}^ν and by the lepton mass matrix $M_e = v_d Y_e$ analytically.

6.1 Analytic Results for Neutrino Masses, Lepton Mixings and CP Phases

The mixing matrix in the lepton sector, the MNS matrix U_{MNS} , is defined by the charged electroweak current $\bar{e}_L^f \gamma^\mu U_{\text{MNS}} \nu_L^f$ in the mass basis. Defining the diagonalization matrices U_{e_L}, U_{e_R} and U_{ν_L} by

$$U_{e_L} M_e U_{e_R}^\dagger = \begin{pmatrix} m_e & 0 & 0 \\ 0 & m_\mu & 0 \\ 0 & 0 & m_\tau \end{pmatrix}, \quad U_{\nu_L} m_{\text{LL}}^\nu U_{\nu_L}^T = \begin{pmatrix} m_1 & 0 & 0 \\ 0 & m_2 & 0 \\ 0 & 0 & m_3 \end{pmatrix}, \quad (41)$$

the MNS matrix is given by

$$U_{\text{MNS}} = U_{e_L} U_{\nu_L}^\dagger. \quad (42)$$

We use the parameterization $U_{\text{MNS}} = R_{23} U_{13} R_{12} P_0$ with R_{23}, U_{13}, R_{12} and P_0 being defined as

$$\begin{aligned} R_{12} &:= \begin{pmatrix} c_{12} & s_{12} & 0 \\ -s_{12} & c_{12} & 0 \\ 0 & 0 & 1 \end{pmatrix}, & U_{13} &:= \begin{pmatrix} c_{13} & 0 & s_{13} e^{-i\delta} \\ 0 & 1 & 0 \\ -s_{13} e^{i\delta} & 0 & c_{13} \end{pmatrix}, \\ R_{23} &:= \begin{pmatrix} 1 & 0 & 0 \\ 0 & c_{23} & s_{23} \\ 0 & -s_{23} & c_{23} \end{pmatrix}, & P_0 &:= \begin{pmatrix} 1 & 0 & 0 \\ 0 & e^{i\beta_2} & 0 \\ 0 & 0 & e^{i\beta_3} \end{pmatrix}. \end{aligned} \quad (43)$$

The masses of the charged leptons are given by $m_\tau = h \varepsilon'_3 v_d$, $m_\mu = e \varepsilon'_2 v_d$ and $m_e = a \varepsilon'_1 v_d$. Unless h, e or a are zero, we can easily choose $\varepsilon'_3, \varepsilon'_2$ and ε'_1 such that the right charged lepton masses are produced. In addition we note that the mixings $\theta_{12}^e, \theta_{13}^e$ and θ_{23}^e , which stem from U_{e_L} and could contribute to the MNS matrix, are very small. Furthermore, in leading order each column of M_e has a common complex phase, which can be absorbed by U_{e_R} . Therefore, the charged leptons do not influence the leptonic CP phases in this approximation.

Using the analytical methods for diagonalizing neutrino mass matrices with small θ_{13} derived in [40], from $m_{\text{LL}}^\nu = m_{\text{LL}}^{\text{II}} + m_{\text{LL}}^{\text{I}}$ we find for the mixing angles

$$\tan(\theta_{23}) \approx \frac{|e|}{|f|}, \quad (44a)$$

$$\tan(2\theta_{13}) \approx \frac{2|a| \varepsilon_1^2 v_u^2 |\sin(\theta_{23})| |b| + \cos(\theta_{23}) |c| \text{sign}(bc e f)}{X |2m_{\text{LL}}^{\text{II}} \sin(\tilde{\delta}) + m_3^{\text{I}} e^{i(2\delta_2 + 3\pi/2 - \tilde{\delta})}|}, \quad (44b)$$

$$\tan(\theta_{12}) \approx \frac{|a|}{|\cos(\theta_{23})| |b| - \sin(\theta_{23}) |c| \text{sign}(bc e f)}, \quad (44c)$$

where m_i^I ($i \in \{1, 2, 3\}$) are the mass eigenvalues of the hierarchical m_{LL}^I given by

$$m_1^I = \mathcal{O}\left(\frac{\varepsilon_3^2 v_u^2}{X'}\right) \approx 0, \quad (45a)$$

$$m_2^I \approx \frac{(|a|^2 + |\cos(\theta_{23})| |b| - \sin(\theta_{23}) |c| \text{sign}(bc e f))^2 \varepsilon_1^2 v_u^2}{X} \approx \frac{|a|^2 \varepsilon_1^2 v_u^2}{\sin^2(\theta_{12}) X}, \quad (45b)$$

$$m_3^I \approx \frac{(|e| \sin(\theta_{23}) + |f| \cos(\theta_{23}))^2 \varepsilon_2^2 v_u^2}{Y}, \quad (45c)$$

and with $\tilde{\delta}$ defined by

$$\tan(\tilde{\delta}) := \frac{m_3^I \sin(2\delta_2 - 2\delta_1)}{m_3^I \cos(2\delta_2 - 2\delta_1) - 2 m^{\text{II}} \cos(2\delta_1)}. \quad (46)$$

Given $\tan(\tilde{\delta})$, $\tilde{\delta}$ has to be chosen such that

$$\frac{\sin(\theta_{23}) |b| + \cos(\theta_{23}) |c| \text{sign}(bc e f)}{\text{sign}(ab) [2 m^{\text{II}} e^{-i(2\delta_1 + 3\pi/2)} \sin(\tilde{\delta}) + m_3^I e^{-i(2\delta_1 - 2\delta_2 + \tilde{\delta})}]} \geq 0. \quad (47)$$

This does not effect θ_{13} , which we have defined to be ≥ 0 , however it is relevant for extracting the Dirac CP phase δ , given by

$$\delta \approx \begin{cases} \tilde{\delta} & \text{for } P \geq 0, \\ \tilde{\delta} + \pi & \text{for } P < 0, \end{cases} \quad (48)$$

with P being defined by

$$P := \frac{\cos(\theta_{23}) |b| - \sin(\theta_{23}) |c| \text{sign}(bc e f)}{\text{sign}(ab) [(\cos(\theta_{23}) |b| - \sin(\theta_{23}) |c| \text{sign}(bc e f))^2 - |a|^2]}. \quad (49)$$

The mass eigenvalues of the complete type II neutrino mass matrix are given by

$$m_1 \approx |m^{\text{II}}|, \quad (50a)$$

$$m_2 \approx |m^{\text{II}} - m_2^I e^{i2\delta_1}|, \quad (50b)$$

$$m_3 \approx |m^{\text{II}} - m_3^I e^{i2\delta_2}|, \quad (50c)$$

and, for $m^{\text{II}} \neq 0$, the Majorana phases β_2 and β_3 can be extracted by

$$\beta_2 \approx \frac{1}{2} \arg(m^{\text{II}} - m_2^I e^{i2\delta_1}), \quad (51a)$$

$$\beta_3 \approx \frac{1}{2} \arg(m^{\text{II}} - m_3^I e^{i2\delta_2}). \quad (51b)$$

A graphical illustration of the correlation between the masses and phases is given in figure 3.

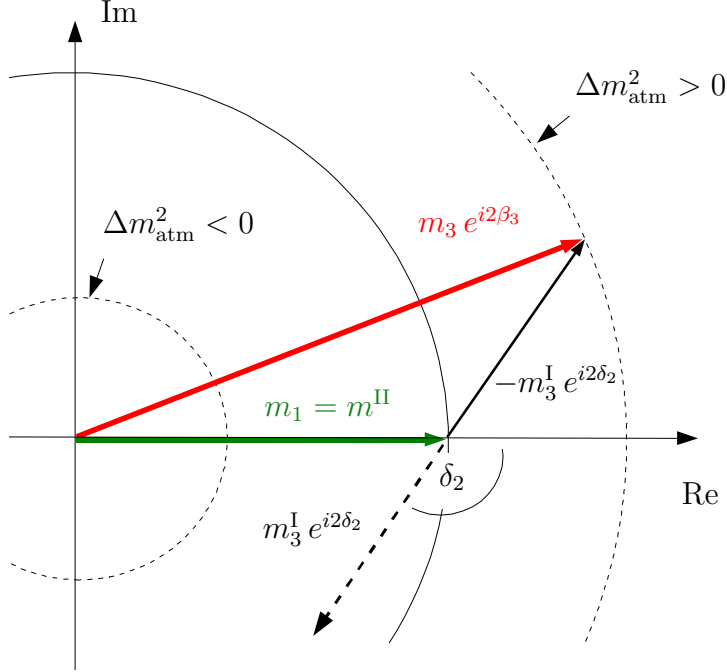


Figure 3: Graphical illustration of how m_3^I has to be chosen in order to produce the experimentally observed atmospheric mass squared difference Δm_{atm}^2 . In the complex plane, $m_3 e^{i2\beta_3} = m_1 - m_3^I e^{i2\delta_2}$ has to lie on one of the dashed circles which correspond to values of m_3 such that the right $|\Delta m_{\text{atm}}^2| := |m_3^2 - m_1^2|$ is produced. The outer dashed circle corresponds to $\Delta m_{\text{atm}}^2 > 0$ and a so-called normal mass ordering $m_3 > m_1$, while the inner dashed circle corresponds to $\Delta m_{\text{atm}}^2 < 0$ and an inverse ordering $m_3 < m_1$. An analogous picture can be drawn for $m_2 e^{i2\beta_2} = m_1 - m_2^I e^{i2\delta_1}$. Note that for Δm_{sol}^2 and θ_{12} , only the combinations $\Delta m_{\text{sol}}^2 > 0$ with $\theta_{12} < 45^\circ$ and $\Delta m_{\text{sol}}^2 < 0$ with $\theta_{12} > 45^\circ$ are allowed by experiment. From the low energy point of view the two possibilities are equivalent, however they correspond to different model parameters at high energy.

6.2 Discussion

We find that for the mixings, only θ_{13} is affected by the direct mass term proportional to the unit matrix, whereas θ_{12} and θ_{23} are independent of m^{II} . This is due to the fact that θ_{23} only depends on the dominant contribution to the type I part of the neutrino mass matrix and θ_{12} depends only on the subdominant type I part to leading order in θ_{13} . On the other hand, θ_{13} depends on both, the dominant and the subdominant part. Looking at equation (44b) for θ_{13} , it naively seems as θ_{13} goes to zero as m^{II} increases. However, by using the result for $\tilde{\delta}$, the denominator of equation (44b) can be rewritten as

$$|2 m^{\text{II}} \sin(\tilde{\delta}) + m_3^I e^{i(2\delta_2 + 3\pi/2 - \tilde{\delta})}| = \left| m_3^I \frac{\cos(2\delta_2 - \tilde{\delta})}{\cos(2\delta_1)} \right|, \quad (52)$$

which does no longer depend on m^{II} explicitly. Note that the term $\cos(2\delta_2 - \tilde{\delta})/\cos(2\delta_1)$ goes to 1 for small m^{II} and to $\cos(2\delta_2)/\cos(2\delta_1)$ for large m^{II} , because $\tilde{\delta}$ goes to 0 as discussed later and is shown in figure 7.¹ Besides the additional explicit dependence on the parameters a, b and c , the mixing angle θ_{13} is only suppressed by a factor of $m_2^{\text{I}}/m_3^{\text{I}}$. However, as we discuss later and is shown in figure 5, m_2^{I} gets smaller for increasing m^{II} much faster than m_3^{I} . Consequently, θ_{13} in fact decreases with increasing m^{II} , however it does not go to zero for large m^{II} . The dependence of θ_{13} on the type II mass scale is illustrated in figure 4.

As the type II contribution $m_{\text{LL}}^{\text{II}}$ gets larger and the neutrino mass scale increases, the mass splittings have to get smaller (see e.g. figure 1) in order to match the experimentally observed mass squared differences $\Delta m_{\text{sol}}^2 := m_2^2 - m_1^2$ and $|\Delta m_{\text{atm}}^2| := |m_3^2 - m_1^2|$. Depending on m^{II} and the complex phases δ_1 and δ_2 , this determines the eigenvalues m_2^{I} and m_3^{I} of the type I part of the neutrino mass matrix (see figure 3). Note that with a hierarchical type I part m_{LL}^{I} , a normal mass ordering as well as an inverse ordering can be achieved. The latter is only possible if $(m^{\text{II}} \cos(2\delta_2))^2 > |\Delta m_{\text{atm}}^2|$. The dependence of m_2^{I} and m_3^{I} on the type II mass scale m^{II} is shown in figure 5. For producing the small mass squared differences for a larger m^{II} in a natural way, i.e. without cancellations of two relatively large terms m_{LL}^{I} and $m_{\text{LL}}^{\text{II}}$, m_2^{I} and m_3^{I} have to be smaller. From equation (50) and the definitions of m_2^{I} and m_3^{I} we find that the masses Y and X of the righthanded neutrinos, which control these mass splittings, can be chosen appropriately in a natural way. As we have already noted, the ratio $m_2^{\text{I}}/m_3^{\text{I}}$ for a partially degenerate mass spectrum is smaller than for hierarchical neutrino masses. This means that in the type II scenario with partially degenerate neutrino masses, sequential righthanded neutrino dominance is even more natural than in the pure type I see-saw case.

As can be seen from equation (51), the m^{II} -dependence of m_2^{I} and m_3^{I} implies that the Majorana phases β_1 and β_2 get smaller for larger m^{II} (see figure 6). From equations (46) and (48), we conclude that the Dirac CP phase δ generically gets smaller for larger m^{II} as well. Quantitatively, the dependence of δ on the type II mass scale is shown in figure 7 for some sample choices of δ_1 and δ_2 .

¹Note that there are special choices of the complex phases where mass eigenvalues of the type I part of the neutrino mass matrix do not become smaller for larger m^{II} . This is e.g. the case for $\delta_2 = 45^\circ$, as can be seen from figure 3. In this case $\tilde{\delta}$ does not go to zero as m^{II} increases. For large m^{II} , we regard this special choices for the phases as unnatural, since two large quantities from m_{LL}^{I} and $m_{\text{LL}}^{\text{II}}$ have to conspire in order to produce a small mass squared difference.

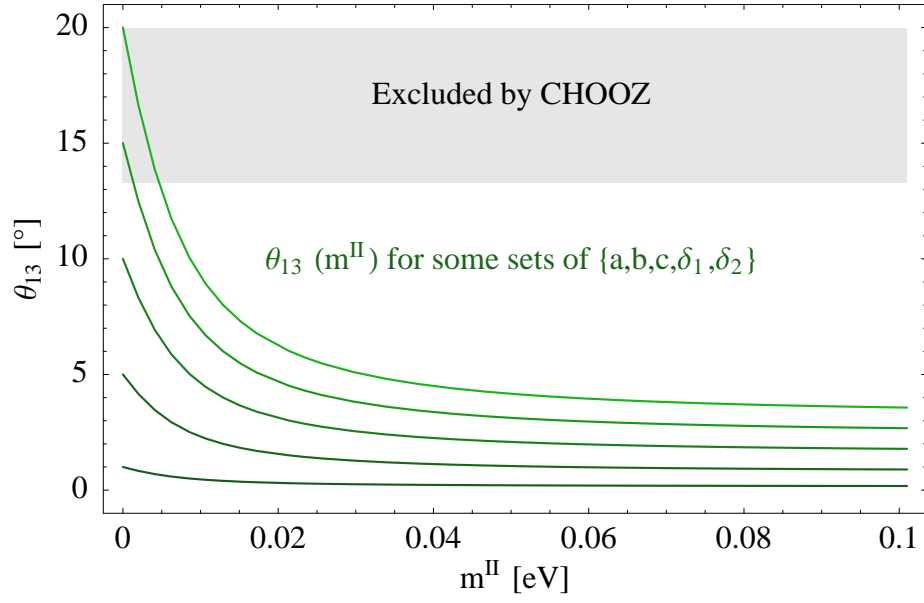


Figure 4: Dependence of θ_{13} on the type II mass scale m^{II} for some sets of parameters $\{a, b, c, \delta_1, \delta_2\}$. Adding the unit matrix contribution $m_{\text{LL}}^{\text{II}} = m^{\text{II}}\mathbb{1}$ leads to a decrease of θ_{13} as m^{II} increases. The grey range for θ_{13} is excluded by experiment at 3σ .

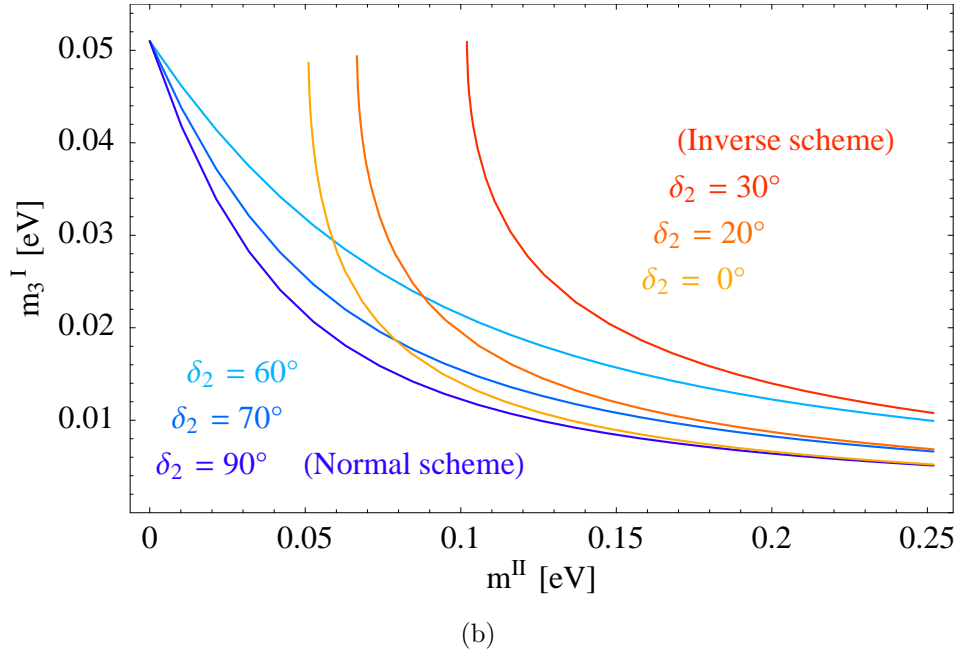
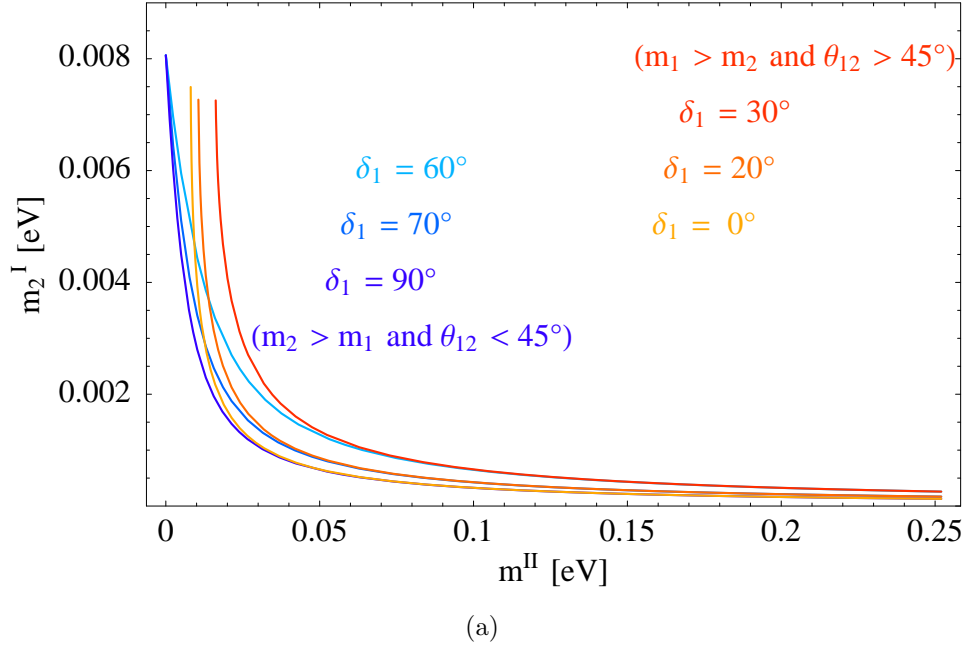
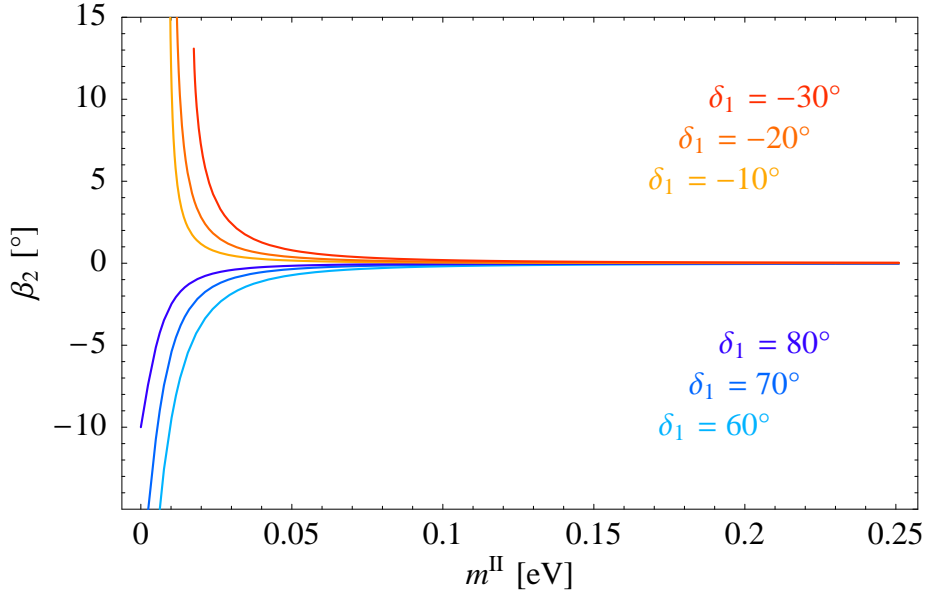
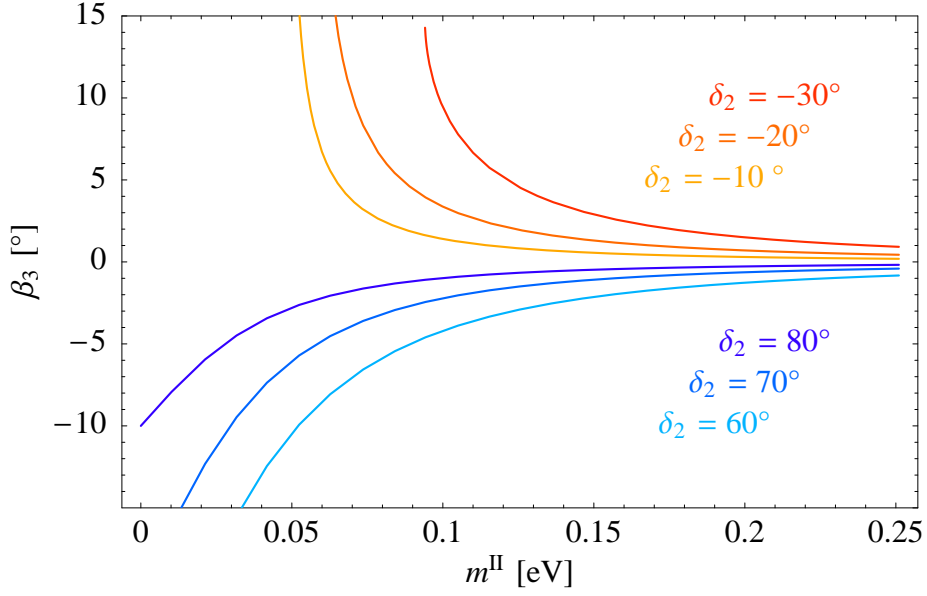


Figure 5: Values for m_2^I and m_3^I as functions of m^{II} , required in order to produce the best-fit values $\Delta m_{\text{atm}}^2 \approx 2.6 \cdot 10^{-3}$ and $\Delta m_{\text{sol}}^2 \approx 6.9 \cdot 10^{-5}$ for some typical choices of the complex phases δ_1 and δ_2 . For a graphical illustration how m_2^I and m_3^I are determined, see figure 3.



(a)



(b)

Figure 6: Diagram (a) shows the dependence of the Majorana CP phase β_2 on m^{II} for some typical values for the complex phase δ_1 and with $\delta_2 = 90^\circ$. Diagram (b) shows the Majorana CP phase β_3 as a function of m^{II} for some sample values δ_2 and with $\delta_1 = 90^\circ$. We see that both phases get smaller for larger m^{II} . The CP phase β_2 is below 5° already for m^{II} larger than about 0.03 eV.

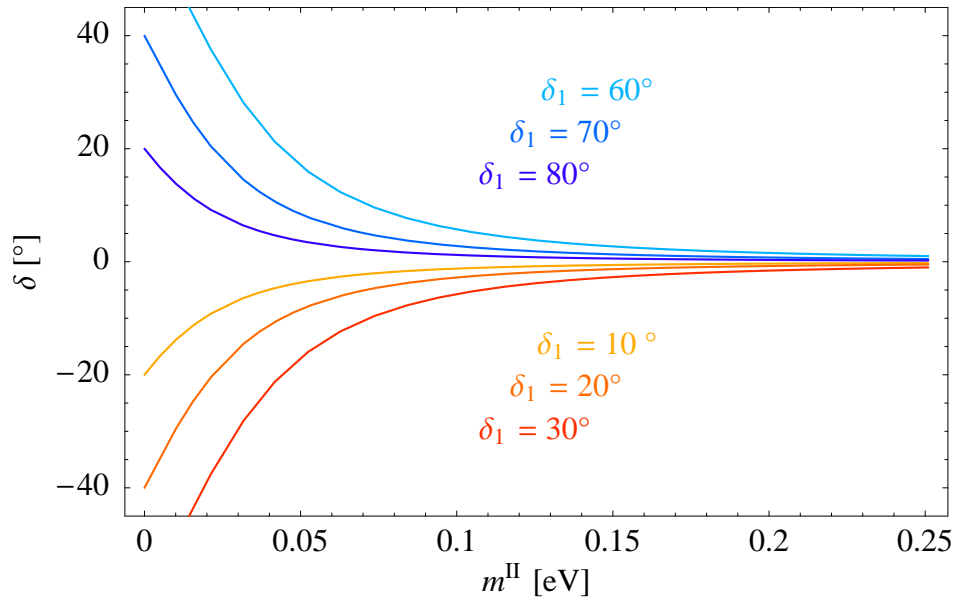


Figure 7: Dependence of the Dirac CP phase δ on m^{II} for some typical values for the complex phase δ_1 and with $\delta_2 = 90^\circ$. A large type II mass scale m^{II} generically implies a small Dirac CP phase.

7 Renormalization Group Corrections

In order to compare the predictions of see-saw scenarios with the experimental data obtained at low energy, the renormalization group (RG) running of the effective neutrino mass matrix has to be taken into account. It is known that for partially degenerate neutrino masses, RG corrections to the neutrino mixing angles can be significant. The corrections to the masses and mass squared differences are relevant even for strongly hierarchical neutrino masses and they can be enhanced or suppressed for a partially degenerate neutrino mass spectrum depending on the CP phases.

Let us assume for example that the considered type II scenarios are embedded into a unified model where all additional degrees of freedom except for the ones contained in the right-handed neutrino superfields $\hat{\nu}_R^i$ are integrated out above some energy scale M_U . At M_U , which could be the scale of gauge coupling unification, the model parameters are defined. In this case, the effective neutrino mass matrix has to be run from M_U to low energy using the β -functions for the various energy ranges above and between the see-saw scales [52, 53] and below the mass scale of the lightest right-handed neutrino [54, 55, 56, 57, 53].

For an accurate computation of the RG corrections for the neutrino mass parameters, the coupled system of differential equations has to be solved successively for the various effective theories [58, 52]. In addition to the parameters of the MNS matrix, the RG running between M_U and the electroweak scale M_{EW} then depends on the additional degrees of freedom corresponding to the lepton Yukawa couplings and the masses of the right-handed neutrinos.

For a small difference of the Majorana CP phases corresponding to the mass eigenvalues m_1 and m_2 , which is generically the case in the presented type II framework, radiative corrections to the lepton mixings have a characteristic property, as has been pointed out in [59, 60]. The running of the solar mixing θ_{12} is generically larger than the RG corrections to the other mixings, if the atmospheric mixing is large already at high energy. We will see that in particular θ_{12} can be significantly lower at high energy, depending on m^H and $\tan\beta$.

We will now estimate the generic size of the RG corrections for the mixing angles by making additional simplifications and assumptions. At first, let us consider the case that the heaviest right-handed neutrino corresponds to the column of the neutrino Yukawa matrix with the largest entries and that it has a mass larger than $M_U \approx 2 \cdot 10^{16}$. If we then assume that the other entries of the neutrino Yukawa matrix are very small compared to y_τ , we can approximately neglect the running due to the neutrino Yukawa matrix and, for a rough estimate, simply use the RGEs for the neutrino mass operator below the see-saw scales. In order to see which quantities control the size of the RG effects, it is useful to consider the RGEs for the parameters of the MNS matrix [61, 62, 63]. For example, the running of the mixing angles in leading order in the small quantity θ_{13} in the MSSM is given by [63]

$$\frac{d}{dt} \theta_{12} = -\frac{y_\tau^2}{32\pi^2} \sin 2\theta_{12} s_{23}^2 \frac{|m_1 + m_2 e^{i2\beta_2}|^2}{\Delta m_{\text{sol}}^2} + \mathcal{O}(\theta_{13}), \quad (53)$$

$$\begin{aligned} \frac{d}{dt} \theta_{13} &= \frac{y_\tau^2}{32\pi^2} \sin 2\theta_{12} \sin 2\theta_{23} \frac{m_3}{\Delta m_{\text{atm}}^2 (1 + \zeta)} \times \\ &\quad \times [m_1 \cos(2\beta_3 - \delta) - (1 + \zeta) m_2 \cos(2\beta_3 - 2\beta_2 - \delta) - \zeta m_3 \cos \delta] \\ &\quad + \mathcal{O}(\theta_{13}), \end{aligned} \quad (54)$$

$$\begin{aligned} \frac{d}{dt} \theta_{23} &= -\frac{y_\tau^2}{32\pi^2} \sin 2\theta_{23} \frac{1}{\Delta m_{\text{atm}}^2} \left[c_{12}^2 |m_2 e^{i2(\beta_3 - \beta_2)} + m_3|^2 + s_{12}^2 \frac{|m_1 e^{i2\beta_3} + m_3|^2}{1 + \zeta} \right] \\ &\quad + \mathcal{O}(\theta_{13}), \end{aligned} \quad (55)$$

where, with the renormalization scale μ , t is defined by $t := \ln(\mu/\mu_0)$ and where we have used the abbreviation $\zeta := \Delta m_{\text{sol}}^2/\Delta m_{\text{atm}}^2$. Compared to the SM, y_τ in the MSSM is given by $y_\tau = y_\tau^{\text{SM}} \sqrt{1 + \tan^2 \beta}$, which yields an enhancement of the RG effects for large $\tan \beta$. In addition, the running is generically enhanced due to factors of the type $m_i^2/\Delta m_{\text{sol}}^2$ or $m_i^2/\Delta m_{\text{atm}}^2$ if the neutrino mass scale is larger than the mass differences. For partially degenerate neutrinos, this is in particular the case for $m_i^2/\Delta m_{\text{sol}}^2$, which enhances the running of θ_{12} .

For an estimate of the RG corrections, we have solved the evolution of the parameters numerically from low energy to high energy under the additional assumptions that $\theta_{13}|_{M_{\text{EW}}} = 0^\circ$ and $\beta_3|_{M_{\text{EW}}} = \beta_2|_{M_{\text{EW}}} = 0^\circ$. Below the SUSY breaking scale, which we have taken to be 1 TeV, we assume the theory to be effectively the Standard Model. The values for $\theta_{12}|_{M_U}$ and $\theta_{23}|_{M_U}$ required in order to produce the best fit value $\theta_{12}|_{M_{\text{EW}}} \approx 32^\circ$ and $\theta_{23}|_{M_{\text{EW}}} \approx 45^\circ$ are shown in figure 8. The RG correction factors for Δm_{sol}^2 and Δm_{atm}^2 with respect to the low energy values $\Delta m_{\text{sol}}^2 \approx 6.9 \cdot 10^{-5} \text{ eV}^2$ and $\Delta m_{\text{atm}}^2 \approx 2.6 \cdot 10^{-3} \text{ eV}^2$ are shown in figure 9 for the case of a normal mass ordering, i.e. $\Delta m_{\text{atm}}^2 > 0$.

It is known that instability under radiative corrections can require unnatural fine-tuning of the high energy parameters in order to produce the experimentally observed mass squared differences and mixings at low energy. Indeed, this is the case for nearly degenerate neutrino masses close to the experimental upper bounds and in addition large $\tan \beta$, such that the slopes $\frac{d}{dt} \theta_{12}$ and $\frac{d}{dt} \Delta m_{\text{sol}}^2$ become very large. As we can see from figures 8 and 9, for the considered ranges of $\tan \beta \in [5, 50]$ and $m^{\text{II}} \in [0.03, 1.5] \text{ eV}$, the RG corrections are well behaved and do not require any fine-tuning of the high energy parameters. Depending on $\tan \beta$, the RG effects for a given neutrino mass scale can either lead to significantly changed values for the mixings and mass squared difference at high energy or cause only rather small corrections. We conclude that though the requirement of naturalness restricts the neutrino mass scale for a given $\tan \beta$ via stability arguments in our scenarios, this does not lead to any problems for partially degenerate neutrinos. Nevertheless, the running has to be included in a careful analysis and it can easily be estimated using the figures 8 and 9.

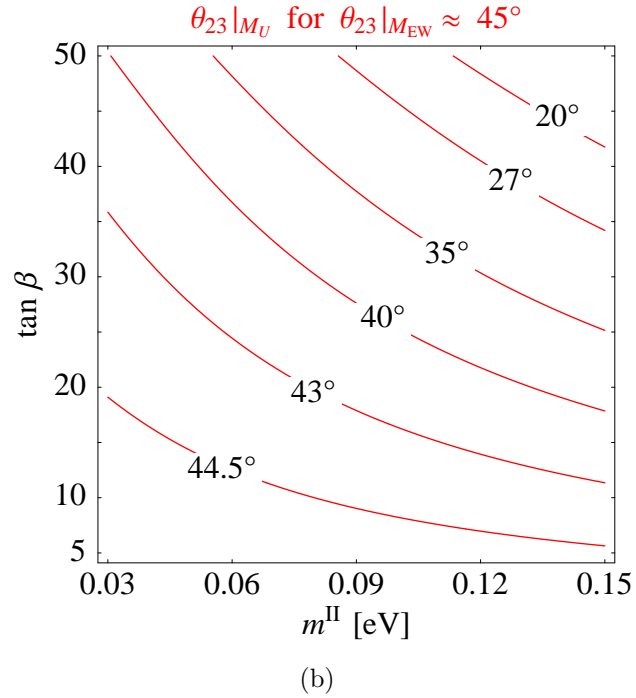
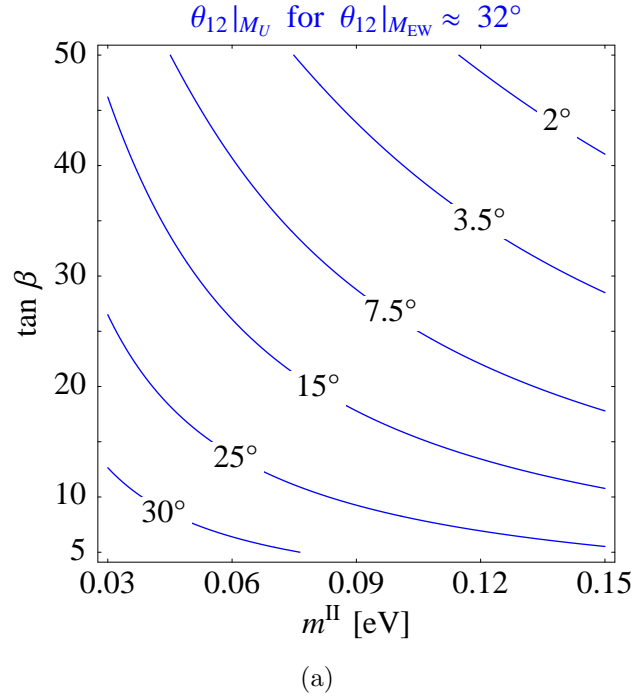


Figure 8: RG corrected values $\theta_{12}|_{M_U}$ and $\theta_{23}|_{M_U}$ at high energy, required in order to produce the best-fit values $\theta_{12} \approx 32^\circ$ and $\theta_{23} \approx 45^\circ$ at low energy M_{EW} . We have considered the case of a normal mass ordering, i.e. $\Delta m_{atm}^2 > 0$. The used approximations and assumptions are explained in the text.

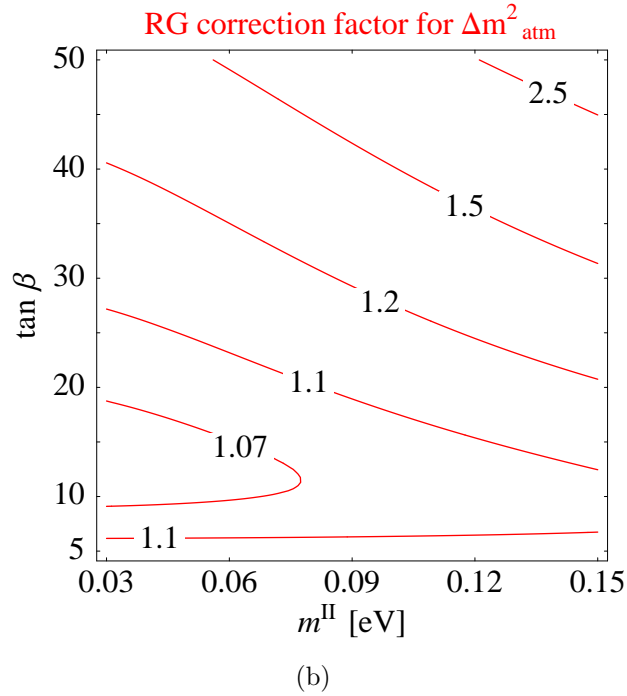
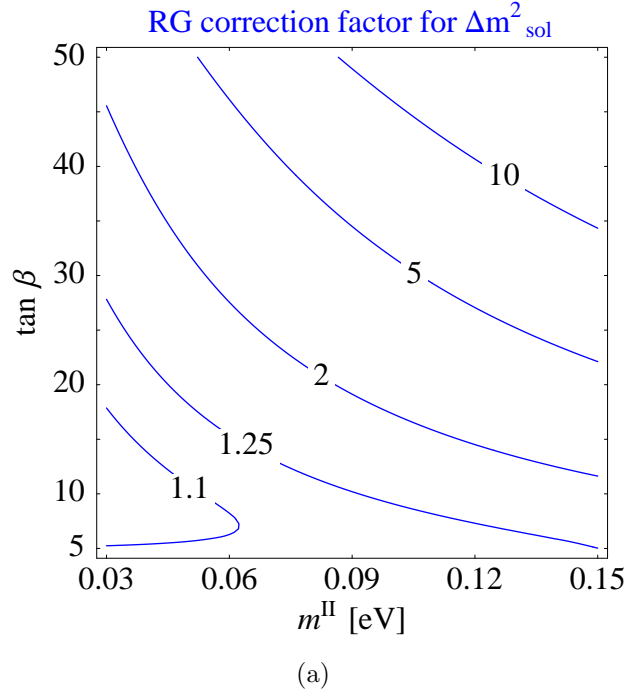


Figure 9: RG correction factors for $\Delta m_{\text{sol}}^2|_{M_U}$ and $\Delta m_{\text{atm}}^2|_{M_U}$ with respect to the low energy best-fit values for the case of a normal mass ordering, i.e. $\Delta m_{\text{atm}}^2 > 0$. For the parameter region shown in the plots, both mass squared differences are larger at high energy. The used approximations and assumptions are explained in the text.

8 Neutrinoless Double Beta Decay

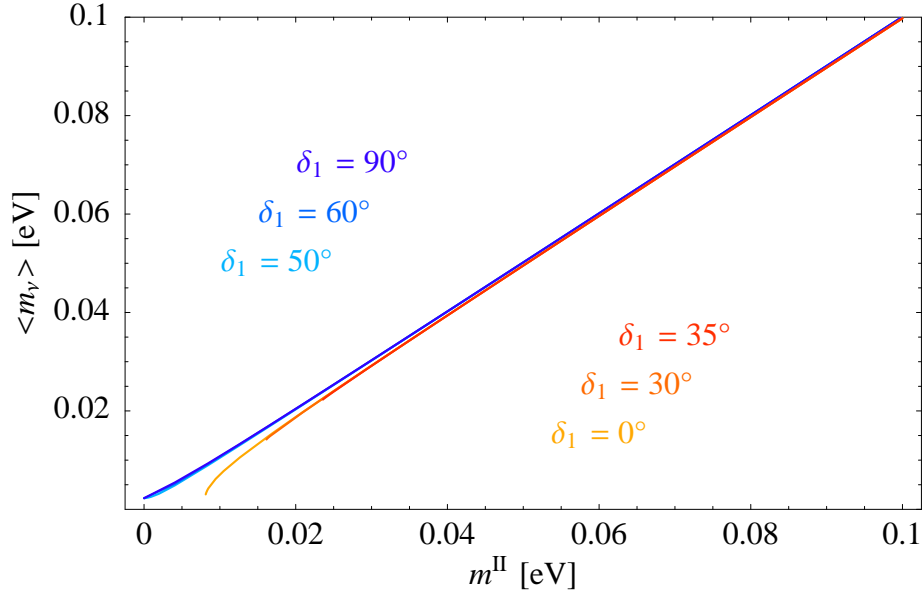
We now discuss the implications of the type II see-saw scenarios with spontaneously broken SO(3) flavour symmetry for $00\nu\beta$ decay. In order to be explicit, we focus on the models of type A1 and B1 with sequential right-handed neutrino dominance and vacuum alignment as introduced in section 6. The effective mass $\langle m_\nu \rangle$ for $00\nu\beta$ decay is then given by

$$\langle m_\nu \rangle = \left| \sum_i (U_{\text{MNS}})_{1i}^2 m_i \right| = |(m_{\text{LL}}^\nu)_{11}| \approx |m^{\text{II}} - \sin^2(\theta_{12}) m_2^{\text{I}} e^{2i\delta_1}|, \quad (56)$$

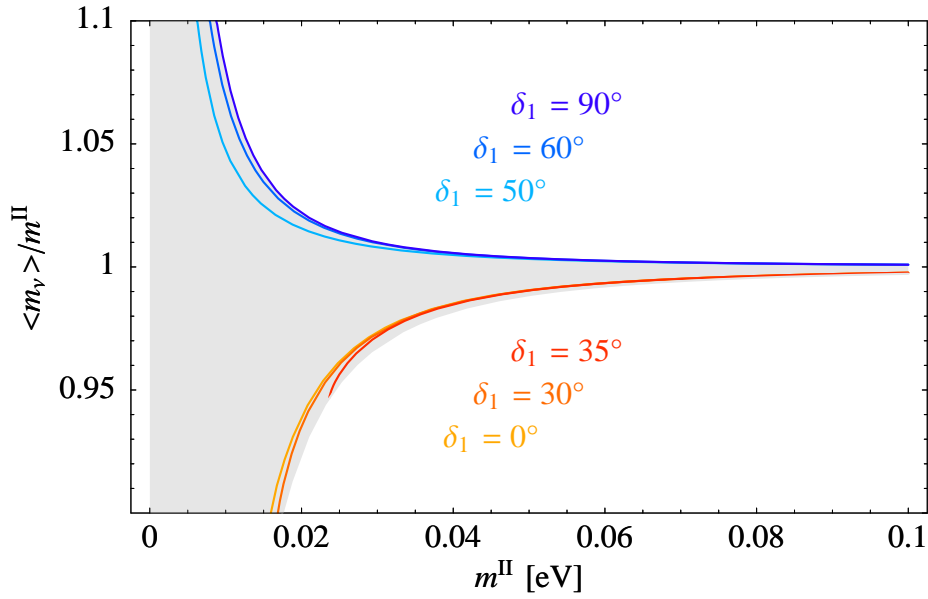
as can be seen from equations (40) and (45b). A discussion of the RG corrections to $\langle m_\nu \rangle$ can be found in [63]. The dependence of $\langle m_\nu \rangle$ on the direct mass term $m_\nu^{\text{II}} = m^{\text{II}}\mathbb{1}$ and on the complex phase δ_1 is illustrated in figure 10. For the models A1 and B1, we obtain $\langle m_\nu \rangle \approx m_\nu^{\text{II}}$ already for a lightest neutrino mass of about 0.02 eV. For all the models with a real vacuum alignment, the general statement holds that when the direct mass term $m^{\text{II}}\mathbb{1}$ becomes dominant over the type I part of the mass matrix, the effective mass $\langle m_\nu \rangle$ is approximately given by m^{II} . The cancellations which can occur in the presence of a large difference of the Majorana phases associated with m_1 and m_2 are then absent and thus there are good prospects for detecting $\langle m_\nu \rangle$ in these classes of type II see-saw models.

9 Discussion and Conclusions

We have proposed a type II upgrade of type I see-saw models leading to new classes of models where partially degenerate neutrinos are as natural as hierarchical ones. A spontaneously broken SO(3) flavour symmetry forces the direct mass term for the neutrinos to be proportional to the unit matrix at leading order. This allows in principle to boost the mass of the lightest neutrino to any desired value leading from hierarchical to nearly degenerate mass spectra. Naturalness of models with nearly degenerate neutrino masses consists of two issues: First there is tree-level naturalness, which means that all parameters and in particular the small mass squared differences and bi-large mixing are produced by the model in a natural way. We have shown that our framework is natural in this respect and could produce any desired level of degeneracy at tree-level. Second, there is naturalness with respect to RG corrections. The latter should not require fine-tuning of the high-energy model parameters in order to produce the low-energy experimental values. RG corrections are un-suppressed in our scenario and thus, depending on $\tan\beta$, the naturalness requirement restricts the neutrino mass scale. Instead of nearly degenerate neutrinos, we have therefore considered partially degenerate neutrinos with a mass scale up to about 0.15 eV, where the running does not lead to



(a)



(b)

Figure 10: The diagrams (a) and (b) show the effective mass $\langle m_\nu \rangle$ for neutrinoless double beta decay and the ratio $\langle m_\nu \rangle / m^{\text{II}}$ as functions of the type II mass scale m^{II} for some typical choices of the complex phase δ_1 in models of type A1 and B1 (see table 4). For other values of δ_1 , the curves lie within the grey region of diagram (b). We see that $\langle m_\nu \rangle \approx m^{\text{II}}$ already for m^{II} larger than about 0.02 eV. We have required that the best-fit value for the solar mass squared difference Δm_{sol}^2 is produced in a natural way, i.e. without cancellation of two large terms in equation (56), and we have used the best-fit experimental value for θ_{12} .

any naturalness problems. This mass range is particularly interesting since it might be accessible to experiments on neutrinoless double beta decay.

For breaking the $SO(3)$ flavour symmetry, we have considered a minimal set of flavon fields and a real alignment mechanism for their $SO(3)$ -breaking vevs. The real vacuum alignment implies that there exists a basis where the Yukawa matrices have three texture zeros. This leads to classes of type II see-saw models with either small mixing from the charged leptons (type A), almost maximal atmospheric mixing from the charged leptons (type B) or models where in principle all mixing can be produced via the charged lepton mass matrix (type C). Characteristic features of them are that each column of the Yukawa matrices has a common complex phase and that, without additional symmetries, the non-zero components of each column have a common typical order of magnitude. In addition, for partially degenerate neutrino masses where the type II contribution m^{II} dominates over the type I part, the Majorana phases associated with the neutrino mass eigenvalues are predicted to be small and the effective mass for neutrinoless double beta decay is approximately given by m^{II} . Future experiments on neutrinoless double beta decay can thus in principle rule out or confirm partially degenerate neutrino masses in this framework.

Bi-large neutrino mixing and the two small mass squared differences can naturally be realized with sequential right-handed neutrino dominance [39, 40] for the type I contribution to the neutrino mass matrix. One of the right-handed neutrinos and the corresponding column of the neutrino Yukawa matrix gives the dominant contribution to the type I mass matrix and is responsible for the large atmospheric mixing θ_{23} and the mass squared difference $\Delta m_{\text{atm}}^2 := m_3^2 - m_1^2$. The subdominant right-handed neutrino and the corresponding column then generate the smaller mass squared difference $\Delta m_{\text{sol}}^2 := m_2^2 - m_1^2$ and can account for a large solar neutrino mixing θ_{12} . Due to the small difference of the Majorana phases corresponding to m_1 and m_2 , the RG effects for θ_{12} in see-saw models are generically larger than for the other lepton mixing angles if θ_{23} is large already at high energy [59, 60]. Depending on $\tan \beta$ and the neutrino mass scale, they can be sizable or lead only to rather small corrections. For partially degenerate neutrinos with a mass scale up to about 0.15 eV, the running in general does not cause problems with naturalness, but it allows for a wider range of possible mass and mixing patterns at high energy. A careful analysis has to include RG effects and we have provided figures where estimates for the corrections can easily be read off.

In the classes of type II see-saw models with sequential right-handed neutrino dominance for the type I contribution to the neutrino mass matrix and real vacuum alignment, the solar and the atmospheric neutrino mixings θ_{12} and θ_{23} are independent of the type II mass scale m^{II} and of the complex phases of the neutrino Yukawa matrix. This provides a natural way to upgrade these types of models continuously from hierarchical neutrino mass spectra to partially degenerate ones, while maintaining the predictions for the two large lepton mixings. The mixing angle θ_{13} is generically small and furthermore decreases with increasing neutrino mass scale. In addition, we find that our scenario

predicts that all observable CP phases, i.e. the Dirac CP phase δ relevant for neutrino oscillations and the Majorana CP phases β_2 and β_3 , become small as the neutrino mass scale increases. This implies in particular that the effective mass for neutrinoless double beta decay is approximately equal to the neutrino mass scale and therefore neutrinoless double beta decay will be observable if the neutrino mass spectrum is partially degenerate. In our framework a partially degenerate neutrino mass spectrum is *a priori* as natural as a hierarchical spectrum. If neutrinos are partially degenerate, neutrinoless double beta decay has the potential to measure the neutrino mass scale.

Acknowledgements

We acknowledge support from the PPARC grant PPA/G/O/2002/00468.

References

- [1] CHOOZ, M. Apollonio et al., *Limits on neutrino oscillations from the CHOOZ experiment*, Phys. Lett. **B466** (1999), 415–430, [hep-ex/9907037](#).
- [2] M. Maltoni, T. Schwetz, M. A. Tortola, and J. W. F. Valle, *Status of three-neutrino oscillations after the SNO-salt data*, (2003), [hep-ph/0309130](#).
- [3] SuperKamiokande, T. Toshito, *Super-Kamiokande atmospheric neutrino results*, (2001), [hep-ex/0105023](#).
- [4] KamLAND, K. Eguchi et al., *First results from KamLAND: Evidence for reactor anti-neutrino disappearance*, Phys. Rev. Lett. **90** (2003), 021802, [hep-ex/0212021](#).
- [5] SNO, S. N. Ahmed et al., *Measurement of the total active B-8 solar neutrino flux at the Sudbury Neutrino Observatory with enhanced neutral current sensitivity*, (2003), [nucl-ex/0309004](#).
- [6] D. N. Spergel et al., *First year Wilkinson Microwave Anisotropy Probe (WMAP) observations: Determination of cosmological parameters*, (2003), [astro-ph/0302209](#).
- [7] H. V. Klapdor-Kleingrothaus et al., *Latest results from the Heidelberg-Moscow double-beta-decay experiment*, Eur. Phys. J. **A12** (2001), 147–154, [hep-ph/0103062](#).
- [8] 16EX Collaboration, C. E. Aalseth et al., *The IGEX Ge-76 neutrinoless double-beta decay experiment: Prospects for next generation experiments*, Phys. Rev. **D65** (2002), 092007, [hep-ex/0202026](#).

- [9] T. Yanagida, in *Proceedings of the Workshop on the Unified Theory and the Baryon Number in the Universe* (O. Sawada and A. Sugamoto, eds.), KEK, Tsukuba, Japan, 1979, p. 95.
- [10] S. L. Glashow, *The future of elementary particle physics*, in *Proceedings of the 1979 Cargèse Summer Institute on Quarks and Leptons* (M. Lévy, J.-L. Basdevant, D. Speiser, J. Weyers, R. Gastmans, and M. Jacob, eds.), Plenum Press, New York, 1980, pp. 687–713.
- [11] M. Gell-Mann, P. Ramond, and R. Slansky, *Complex spinors and unified theories*, in *Supergravity* (P. van Nieuwenhuizen and D. Z. Freedman, eds.), North Holland, Amsterdam, 1979, p. 315.
- [12] R. N. Mohapatra and G. Senjanović, *Neutrino mass and spontaneous parity violation*, Phys. Rev. Lett. **44** (1980), 912.
- [13] D. O. Caldwell and R. N. Mohapatra, *Neutrino mass explanations of solar and atmospheric neutrino deficits and hot dark matter*, Phys. Rev. **D48** (1993), 3259–3263.
- [14] P. Bamert and C. P. Burgess, *Naturally degenerate neutrinos*, Phys. Lett. **B329** (1994), 289–294, hep-ph/9402229.
- [15] D.-G. Lee and R. N. Mohapatra, *An $SO(10) \times S_4$ scenario for naturally degenerate neutrinos*, Phys. Lett. **B329** (1994), 463–468, hep-ph/9403201.
- [16] A. Ioannisian and J. W. F. Valle, *$SO(10)$ grand unification model for degenerate neutrino masses*, Phys. Lett. **B332** (1994), 93–99, hep-ph/9402333.
- [17] A. S. Joshipura, *Almost degenerate neutrinos*, Z. Phys. **C64** (1994), 31–35.
- [18] A. S. Joshipura, *Degenerate neutrinos in left-right symmetric theory*, Phys. Rev. **D51** (1995), 1321–1325, hep-ph/9404354.
- [19] A. Ghosal, *Almost degenerate neutrino mass in an $SU(2)_{QL} \times SU(2)_{LL} \times U(1)_Y$ model*, Phys. Lett. **B398** (1997), 315–320.
- [20] C. D. Carone and M. Sher, *Supersymmetric model of quasi-degenerate neutrinos*, Phys. Lett. **B420** (1998), 83–90, hep-ph/9711259.
- [21] E. Ma, *Splitting of three nearly mass-degenerate neutrinos*, Phys. Lett. **B456** (1999), 48–53, hep-ph/9812344.
- [22] A. K. Ray and S. Sarkar, *Almost degenerate neutrinos in a left-right symmetric model with discrete symmetries*, Phys. Rev. **D58** (1998), 055010.

- [23] G. Lazarides, *Degenerate neutrinos and supersymmetric inflation*, Phys. Lett. B **452** (1999) 227, hep-ph/9812454.
- [24] C. Wetterich, *Natural maximal ν_μ - ν_τ mixing*, Phys. Lett. **B451** (1999), 397–405, hep-ph/9812426.
- [25] Y.-L. Wu, *$SO(3)$ gauge symmetry and neutrino-lepton flavor physics*, Phys. Rev. **D60** (1999), 073010, hep-ph/9810491.
- [26] A. Ghosal, *Bi-maximal neutrino mixing with $SO(3)$ flavour symmetry*, hep-ph/9905470.
- [27] R. Barbieri, L. J. Hall, G. L. Kane, and G. G. Ross, *Nearly degenerate neutrinos and broken flavour symmetry*, (1999), hep-ph/9901228.
- [28] Y.-L. Wu, *Two/three-flavor oscillation and MSW/just-so solution of neutrinos in the $SO(3)$ gauge model*, Int. J. Mod. Phys. **A14** (1999), 4313–4330, hep-ph/9901320.
- [29] Y.-L. Wu, *Spontaneous breaking of flavor symmetry and naturalness of nearly degenerate neutrino masses and bi-maximal mixing*, Sci. China **A43** (2000), 988–995, hep-ph/9906435.
- [30] E. Ma and G. Rajasekaran, *Softly broken A_4 symmetry for nearly degenerate neutrino masses*, Phys. Rev. **D64** (2001), 113012, hep-ph/0106291.
- [31] K. S. Babu, E. Ma, and J. W. F. Valle, *Underlying A_4 symmetry for the neutrino mass matrix and the quark mixing matrix*, Phys. Lett. **B552** (2003), 207–213, hep-ph/0206292.
- [32] M. Patgiri and N. N. Singh, *Right-handed Majorana neutrino mass matrices for generating bimaximal mixings in degenerate and inverted models of neutrinos*, Int. J. Mod. Phys. **A18** (2003), 743–754, hep-ph/0301254.
- [33] R. N. Mohapatra, M. K. Parida, and G. Rajasekaran, *High scale mixing unification and large neutrino mixing angles*, (2003), hep-ph/0301234.
- [34] G. Lazarides, Q. Shafi and C. Wetterich, *Proton lifetime and fermion masses in an $SO(10)$ model*, Nucl. Phys. B **181** (1981) 287.
- [35] R. N. Mohapatra and G. Senjanović, *Neutrino masses and mixings in gauge models with spontaneous parity violation*, Phys. Rev. **D23** (1981), 165.
- [36] C. Wetterich, *Neutrino masses and the scale of $B - L$ violation*, Nucl. Phys. **B187** (1981), 343.

- [37] E. Ma and U. Sarkar, *Neutrino masses and leptogenesis with heavy Higgs triplets*, Phys. Rev. Lett. **80** (1998), 5716–5719, hep-ph/9802445.
- [38] S. F. King, *Neutrino mass models*, Rept. Prog. Phys. **67** (2004), 107–158, hep-ph/0310204.
- [39] S. F. King, *Large mixing angle MSW and atmospheric neutrinos from single right-handed neutrino dominance and $U(1)$ family symmetry*, Nucl. Phys. **B576** (2000), 85–105, hep-ph/9912492.
- [40] S. F. King, *Constructing the large mixing angle MNS matrix in see-saw models with right-handed neutrino dominance*, JHEP **09** (2002), 011, hep-ph/0204360.
- [41] J. C. Pati and A. Salam, *Lepton number as the fourth color*, Phys. Rev. **D10** (1974), 275–289.
- [42] R. N. Mohapatra and J. C. Pati, *A 'natural' left-right symmetry*, Phys. Rev. **D11** (1975), 2558.
- [43] G. Senjanović and R. N. Mohapatra, *Exact left-right symmetry and spontaneous violation of parity*, Phys. Rev. **D12** (1975), 1502.
- [44] J. C. Pati and A. Salam, *Unified lepton - hadron symmetry and a gauge theory of the basic interactions*, Phys. Rev. **D8** (1973), 1240.
- [45] H. Georgi, *Particles and fields*, (edited by Carlson, C. E.), A.I.P., 1975, p. 575.
- [46] H. Fritzsch and P. Minkowski, *Unified interactions of leptons and hadrons*, Ann. Phys. **93** (1975), 193–266.
- [47] C. D. Froggatt and H. B. Nielsen, *Statistical analysis of quark and lepton masses*, Nucl. Phys. **B164** (1980), 114.
- [48] S. F. King and I. N. R. Peddie, *Canonical normalisation and Yukawa matrices*, (2003), hep-ph/0312237.
- [49] S. F. King, *Atmospheric and solar neutrinos with a heavy singlet*, Phys. Lett. **B439** (1998), 350–356, hep-ph/9806440.
- [50] S. F. King, *Atmospheric and solar neutrinos from single right-handed neutrino dominance and $U(1)$ family symmetry*, Nucl. Phys. **B562** (1999), 57–77, hep-ph/9904210.
- [51] K. S. Babu and S. M. Barr, *Bimaximal neutrino mixings from lopsided mass matrices*, Phys. Lett. **B525** (2002), 289–296, hep-ph/0111215.

- [52] S. Antusch, J. Kersten, M. Lindner, and M. Ratz, *Neutrino mass matrix running for non-degenerate see-saw scales*, Phys. Lett. **B538** (2002), 87–95, [hep-ph/0203233](#).
- [53] S. Antusch and M. Ratz, *Supergraph techniques and two-loop beta-functions for renormalizable and non-renormalizable operators*, JHEP **07** (2002), 059, [hep-ph/0203027](#).
- [54] P. H. Chankowski and Z. Pluciennik, *Renormalization group equations for seesaw neutrino masses*, Phys. Lett. **B316** (1993), 312–317, [hep-ph/9306333](#).
- [55] K. S. Babu, C. N. Leung, and J. Pantaleone, *Renormalization of the neutrino mass operator*, Phys. Lett. **B319** (1993), 191–198, [hep-ph/9309223](#).
- [56] S. Antusch, M. Drees, J. Kersten, M. Lindner, and M. Ratz, *Neutrino mass operator renormalization revisited*, Phys. Lett. **B519** (2001), 238–242, [hep-ph/0108005](#).
- [57] S. Antusch, M. Drees, J. Kersten, M. Lindner, and M. Ratz, *Neutrino mass operator renormalization in Two Higgs Doublet Models and the MSSM*, [hep-ph/0110366](#) (2001).
- [58] S. F. King and N. N. Singh, *Renormalisation group analysis of single right-handed neutrino dominance*, Nucl. Phys. **B591** (2000), 3–25, [hep-ph/0006229](#).
- [59] S. Antusch, J. Kersten, M. Lindner, and M. Ratz, *The LMA solution from bimaximal lepton mixing at the GUT scale by renormalization group running*, Phys. Lett. **B544** (2002), 1–10, [hep-ph/0206078](#).
- [60] S. Antusch and M. Ratz, *Radiative generation of the LMA solution from small solar neutrino mixing at the GUT scale*, JHEP **11** (2002), 010, [hep-ph/0208136](#).
- [61] P. H. Chankowski, W. Krolkowski, and S. Pokorski, *Fixed points in the evolution of neutrino mixings*, Phys. Lett. **B473** (2000), 109, [hep-ph/9910231](#).
- [62] J. A. Casas, J. R. Espinosa, A. Ibarra, and I. Navarro, *General RG equations for physical neutrino parameters and their phenomenological implications*, Nucl. Phys. **B573** (2000), 652, [hep-ph/9910420](#).
- [63] S. Antusch, J. Kersten, M. Lindner, and M. Ratz, *Running neutrino masses, mixings and CP phases: Analytical results and phenomenological consequences*, Nucl. Phys. **B674** (2003), 401–433, [hep-ph/0305273](#).